BIOFUELS PRODUCTION USING CANOLA OIL OVER HETEROGENEOUS CATALYSTS

A Thesis Submitted to
the Graduate School of Engineering and Sciences of
İzmir Institute of Technology
in Partial Fulfillment of the Requirements for the Degree of

MASTER OF SCIENCE

in Chemical Engineering

by
Bertan ÖZDOĞRU

December 2017
İZMİR

We approve the thesis of **Bertan ÖZDOĞRU**

Examining Committee Members:

Prof. Dr. Erol ŞEKER
Department of Chemical Engineering, İzmir Institute of Technology

Asst. Prof. Dr. Ali Can KIZILKAYA
Department of Chemical Engineering, İzmir Institute of Technology

Prof. Dr. Oğuz BAYRAKTAR
Department of Chemical Engineering, Ege University

29 December 2017

Prof. Dr. Erol ŞEKER
Supervisor, Department of Chemical Engineering, İzmir Institute of Technology

Prof. Dr. Erol ŞEKER
Head of the Department of Chemical Engineering

Prof. Dr. Aysun SOFUOĞLU
Dean of the Graduate School of Engineering and Science

ACKNOWLEDGEMENTS

In the beginning of this M.Sc. thesis, it is a necessity for me to show my appreciation to the people whose effort made this thesis possible. To start with, I would like to express my utmost gratitude to my advisor Prof. Dr. Erol Şeker for his guidance, encouragement, and support from the beginning of my M.Sc. study. All the experienced gained throughout this study helped me during research and writing of this thesis and will be carried with me rest of my life.

At this point, I must express special thanks to many of my co-workers, more importantly, friends; Özgün Deliismail, Berk Türkkul, Emre Değirmenci, Orkan Dal, Emre Demirkaya, Okan Akın, Efecan Pakkaner, Mesut Genishoğlu, Meriç Başol, Kemal Barutçu and Merve Uçaroğlu for their support and helpful suggestion throughout the thesis period.

I also would like to thank research specialists Işın Özçelık, Handan Gaygısız, Nesrin Ahıpaşaoğlu and Dr. Gülnihal Yelken for their expertise and support. I should also thank both Izmir Institute of Technology, Center for Materials Research and Izmir Institute of Technology, Center of Environmental Research for providing the facilities necessary for this study.

Finally, this study could not be possible without the support of my family. I would like to appreciate my mother Mihriban Özdoğru, my sister Benay Özdoğru and my nephew Lara Gültekin that their being behind me all the time gave me the strength for going forward.

ABSTRACT

BIOFUELS PRODUCTION USING CANOLA OIL OVER HETEROGENEOUS CATALYSTS

The goal of this study was to investigate the activity of Ni loaded on Al_2O_3-SiO_2 supports prepared with different acids for the production of biofuel grade compounds while using canola oil as our feedstock. While keeping the reaction conditions constant, catalyst preparation parameters such as aluminum concentration, nickel concentration, calcination temperature, and acid types investigated with statistical methods by constructing Box Behnken design using three continuous parameters with two levels and one categorical parameter with three level. Responses considered in this study were aldehyde, ester, organic acid and other compound yields calculated from the GC-MS analysis.

After ANOVA analysis, empirical models calculated from this analysis used to optimize the catalyst preparation parameters. Three catalysts, one for each acid type, selected to investigate the validity of our model. Analysis did on these catalysts have shown that both 0% Ni/25% Al_2O_3-75% SiO_2 w/H_2SO_4 at 900^oC and 20% Ni/75% Al_2O_3-25% SiO_2 w/H_3PO_4 at 900^oC catalysts gave good ester yields with good organic acid utilization. 20% Ni/75% Al_2O_3-25% SiO_2 w/H_3PO_4 at 900^oC catalyst was exceptional in ester selectivity aspect while 0% Ni/25% Al_2O_3-75% SiO_2 w/H_2SO_4 at 900^oC catalyst was in organic acid utilization aspect.

Presence of aluminum phosphate crystal phase observed with XRD resulted in 20% Ni/75% Al_2O_3-25% SiO_2 w/H_3PO_4 at 900^oC catalyst having the highest selectivity towards ester production. Combination of weak and strong acid sites increased the organic acid selectivity while lowering the selectivity towards esters for 0% Ni/25% Al_2O_3-75% SiO_2 w/H_2SO_4 at 900^oC catalyst. From the low organic acid utilization observed with 10% Ni/25% Al_2O_3-75% SiO_2 w/HNO_3 at 500^oC and, 10% Ni/50% Al_2O_3-50% SiO_2 w/H_2SO_4 at 700^oC catalysts which had high amounts of weak acid sites, it could be said that organic acids can only be reacted over strong acid sites.

ÖZET

HETEROJEN KATALİZÖRLER ÜZERİNDE KANOLA YAĞI KULLANARAK BİYOYAKITLARIN ÜRETİMİ

Bu çalışmada farklı asitlerle hazırlanmış Ni yüklü Al_2O_3-SiO_2 desteği üzerine Ni yüklenmesinin sabit reaksiyon koşullarında biyoyakıt üretimi üzerindeki etkisi incelenmiştir. Başlangıç malzemesi olarak kanola yağı kullanılırken, aluminyum miktarı, nikel miktarı, kalsinasyon sıcaklığı ve peptitleme işleminde kullanılan asit tipinin katalizör ve reaksiyon üzerindeki etkisini incelemek için Box Behnken istatistiksel tasarımı kullanılmıştır. Tasarım hazırlanırken devamlı üç değişken için iki seviye seçilirken, kategori değişkeni için üç seviye seçilmiştir. Tasarımın sonuçlarını izlemek için, GC-MS analizlerini kullanarak aldehit, ester, organik asit ve diğer ürünlerin üretim miktarları incelenmiştir.

ANOVA analizleri sonucunda ortaya çıkan model denklemleri kullanılarak, her asit tipi için bir tane olacak şekilde en iyi sonuçları verecek katalizör hazırlama koşulları hesaplanmıştır. Bu katalizörler de biyoyakıt üretimi reaksiyonlarına sokularak modellerin geçerliliği incelenmiştir. Ürün analizleri en yüksek ester seçiciliğini 900°C'de H_3PO_4 asidi ile yapılan %20 Ni/%75 Al_2O_3-%25 SiO_2 katalizörünün verdiğini göstermiştir. En çok organic asidi reaksiyona sokan katalizör ise 900°C'de H_2SO_4 asidi ile hazırlanan %0 Ni/%25 Al_2O_3-%75 SiO_2 katalizörü olmuştur.

XRD analizi göz önüne alındığında, 900°C kalsinasyonda H_3PO_4 asidi kullanılarak hazırlanan %20 Ni/%75 Al_2O_3-%25 SiO_2 katalizörünün ester üretiminin aluminyum fosfat kristal fazından ötürü kaynaklandığı söylenebilir. Kuvvetli ve zayıf asit bölgelerinin birleşimi, 900°C kalsinasyonda H_2SO_4 asidi ile hazırlanan %0 Ni/%25 Al_2O_3-%75 SiO_2 katalizörünün düşük ester seçiciliği ile en fazla organik asidi reaksiyona soktuğu da analizlerin sonunda ortaya çıkmıştır. 500°C'de HNO_3 ile yapılan %10 Ni/%25 Al_2O_3-%75 SiO_2 ve 700°C'de H_2SO_4 ile yapılan %10 Ni/50% Al_2O_3-%50 SiO_2 katalizörlerinin kötü performansı, zayıf asit bölgelerinin organik asit ile reaksiyona girememesinden kaynaklanmaktadır.

TABLE OF CONTENTS

LIST OF FIGURES…… viii

LIST OF TABLES…..... ix

CHAPTER 1. INTRODUCTION 1

CHAPTER 2. LITERATURE SURVEY 9

2.1. Organic Acid Composition of the Vegetable and Animal Oils 9

2.2. Industrial Biofuel Production 11

2.3. Biofuel Production from Acid Heterogeneous Catalysts 13

CHAPTER 3. MATERIALS AND METHODS 21

3.1. Materials 21

3.2. Catalyst Preparation 22

3.3. Biofuel Production with Ni/Al_2O_3-SiO_2 Catalysts 22

3.4. Box Behnken Design for Catalyst Composition Selection 23

3.5. Catalyst Characterization 23

CHAPTER 4. RESULTS AND DISCUSSION 27

4.1.Analysis of Variance Studies for Aldehydes, Esters, Organic Acids and Other Compound Yields 27

4.2. Catalyst Optimization using ANOVA Analysis 35

4.3. Catalyst Characterization 38

4.3.1. X-Ray Diffraction Analysis 38

4.3.2. TPD and BET Analysis 42

CHAPTER 5. CONCLUSION 46

REFERENCES……. 47

APPENDICES

APPENDIX A. GC-MS DETECTED COMPOUND LIST 51

APPENDIX B. RESIDUAL PLOTS 53

APPENDIX C. MODEL COEFFICIENT CALCULATION AND MODEL SUMMARY 55

APPENDIX D. BET ADSORPTION-DESORPTION ISOTHERMS..... 57

APPENDIX E. NH_3-TPD PLOTS 60

LIST OF FIGURES

Figure **Page**

Figure 1.1. Contribution of energy sources in the total energy produced in World (right) and in Turkey (left) at 2016 (Source: BP 2017) 2
Figure 1.2. Atmospheric CO_2 concentration over time (negative values = BCE) 2
Figure 1.3. Crude oil prices between 1861-2016 3
Figure 1.4. Total CO_2 emission in the European Union in 1990 (left) and 2015 (right) .. 3
Figure 1.5. Total CO_2 emission in the Turkey in 1990 (left) and 2013 (right) 4
Figure 1.6. Renewable feedstocks and their reaction routes 4
Figure 1.7: Biodiesel transesterification route 6
Figure 1.8. FFA soap production 6
Figure 1.9. Biodiesel esterification route 7
Figure 1.10. Biodiesel deoxygenation route 7
Figure 2.1. Flow diagram of homogeneous alkali catalyzed biodiesel production 12
Figure 2.2. Generation of Bronsted acid site over aluminosilicate 14
Figure 2.3. Generation of Lewis acid site over aluminosilicate 14
Figure 2.4. Reaction list of triglyceride decomposition 14
Figure 4.1. GC-MS final product distribution 37
Figure 4.2. XRD spectra of selected catalysts prepared with HNO_3 40
Figure 4.3. XRD spectra of selected catalysts prepared with H_2SO_4 41
Figure 4.4. XRD spectra of selected catalysts prepared with H_3PO_4 42
Figure 4.5. Product distribution of selected catalysts with their total acid amount 44

LIST OF TABLES

Table **Page**

Table 2.1. Typical fatty acid composition of various vegetable and animal oils 10
Table 2.2. Oil conversion and hydrocarbon selectivity in terms of various heterogeneous acid catalysts and reaction conditions. 16
Table 3.1. List of chemicals used in the synthesis of catalysts and their properties 21
Table 3.2. Names and composition of catalysts prepared with HNO3 24
Table 3.3. Names and composition of catalysts prepared with H2SO4 25
Table 3.4. Names and composition of catalysts prepared with H_3PO_4 25
Table 3.5. List of continuous and categorical factors used in the experimental design . 26
Table 4.1. Box Behnken design and responses as aldehydes, esters, organic acids and others for the catalysts prepared with HNO_3 28
Table 4.2. Box Behnken design and responses as aldehydes, esters, organic acids and others for the catalysts prepared with H_2SO_4 29
Table 4.3. Box Behnken design and responses as aldehydes, esters, organic acids and others for the catalysts prepared with H_3PO_4 30
Table 4.4. Calculated ANOVA analysis for aldehyde yield in the product with two-sided 90% confidence interval 31
Table 4.5. Calculated ANOVA analysis for ester yield in the product with two-sided 90% confidence interval 33
Table 4.6. Calculated ANOVA analysis for organic acid yield in the product with two-sided 90% confidence interval 34
Table 4.7. Calculated ANOVA analysis for other compound yield in the product with two-sided 90% confidence interval 35
Table 4.8. Optimized catalyst preparation conditions to maximize ester production 36
Table 4.9. GC-MS results of optimized catalyst final product distribution 36
Table 4.10. XRD crystal sizes and crystal phases for selected catalysts 39
Table 4.11. BET surface area and average pore volumes of selected catalysts 43

CHAPTER 1

INTRODUCTION

After the discovery of controlled fire, energy sources, as well as energy itself, became one of the most important criteria for mankind to exist out in nature, after food and shelter. Harnessing the power of nature as useful energy with watermills and windmills was the next big step in human evolution. However, the unpredictability of wind and water power meant that in order to continue evolution, new energy sources needed to be found that can be controlled with ease. Steam energy revolutionized the use of energy and started the First Industrial Revolution.

Internal combustion engines (ICE's) were the next big step. Since the requirement of huge steam tanks and water sources can be eliminated, using ICE's were much more practical compared to steam engines. Initially used in automobile and motorbike, they started to replace steam engines. The energy required to run both steam and ICE's came from fossil fuels, such as coal and petroleum.

Nowadays, main source of the energy that run our everyday life comes from fossil fuels, covering 85 % of the total energy production (Coal 28%, petrol 33% and natural gas 24%) and rest distributed between hydroelectricity, nuclear and renewable energy, In Turkey, the numbers are very similar, as fossil fuels produced 85% of the total energy while renewable energy and hydroelectricity produced 4% and 11%, respectively, in the absence of nuclear energy facilities. (Figure 1.1) (BP 2017)

Heavily depending on fossil fuels for the generation of energy has serious environmental, economic and geopolitical consequences that observed from the beginning of 20^{th} century to today. Utilization of nonrenewable energy sources caused air pollution and global warming affecting the whole world, especially developing countries. As it can be seen in Figure 1.2 (left), the air's carbon dioxide (CO_2) concentrations changed between as low as 170 ppm to as much as 300 ppm and these concentration changes occurred between tens of thousands of years. However, starting from 1950's, CO_2 concentrations rapidly increased, reaching 400 ppm level in 2015, shown in Figure 1.2 (right). This, not only changes the whole air ecosystem but also with other combustion

products such as carbon monoxide (CO), nitrogen oxides (NO_x's) and sulfur oxides (SO_x's) results with air pollution, acid rains and global warming,

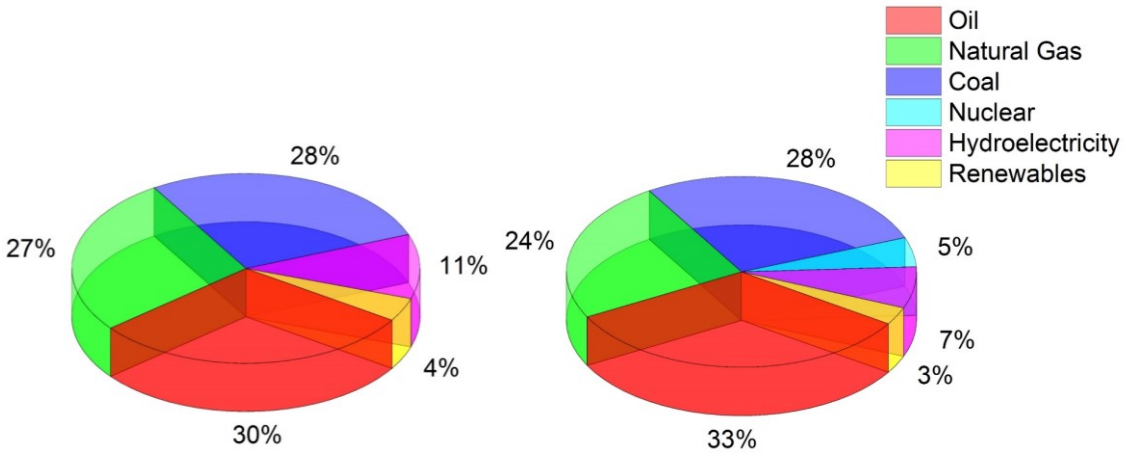

Figure 1.1. Contribution of energy sources in the total energy produced in World (right) and in Turkey (left) at 2016 (Source: BP 2017)

Uncertainty over oil price is another problem with fossil fuel, especially for an energy-dependent country like Turkey. Geopolitical events and market manipulations drastically changed the oil prices throughout the globe over the years. (Figure 1.3) Even a regional event has the possibility of creating a domino effect and can increase the oil prices in the whole world. (BP 2017)

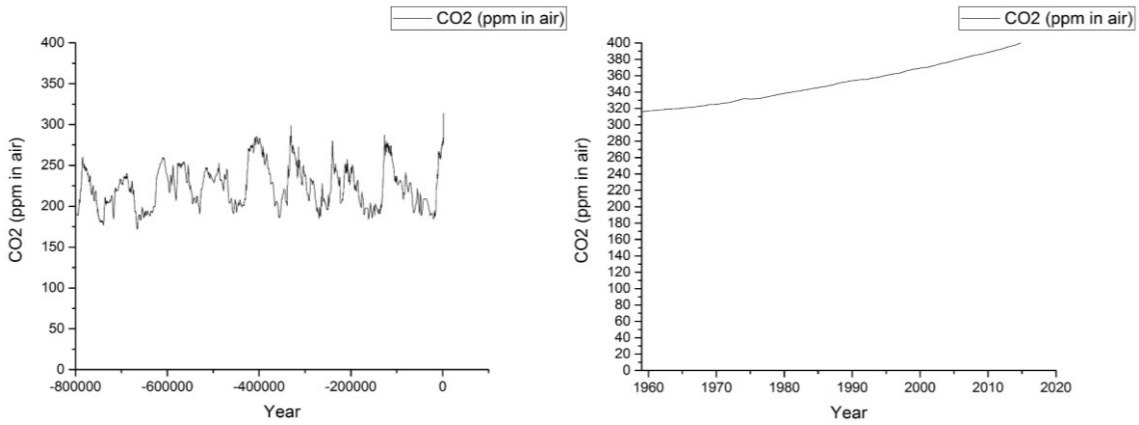

Figure 1.2. Atmospheric CO_2 concentration over time (negative values = BCE) (Source: EPA 2016)

By considering the information mentioned above; environmental pollution and negative health effects, not to mention burden that comes with its economic and geopolitical uncertainties on a developing country like Turkey, reduction of dependence on such energy sources should be prioritized. Our country's potential renewable and alternative energy sources are really good candidates to solve this very problem.

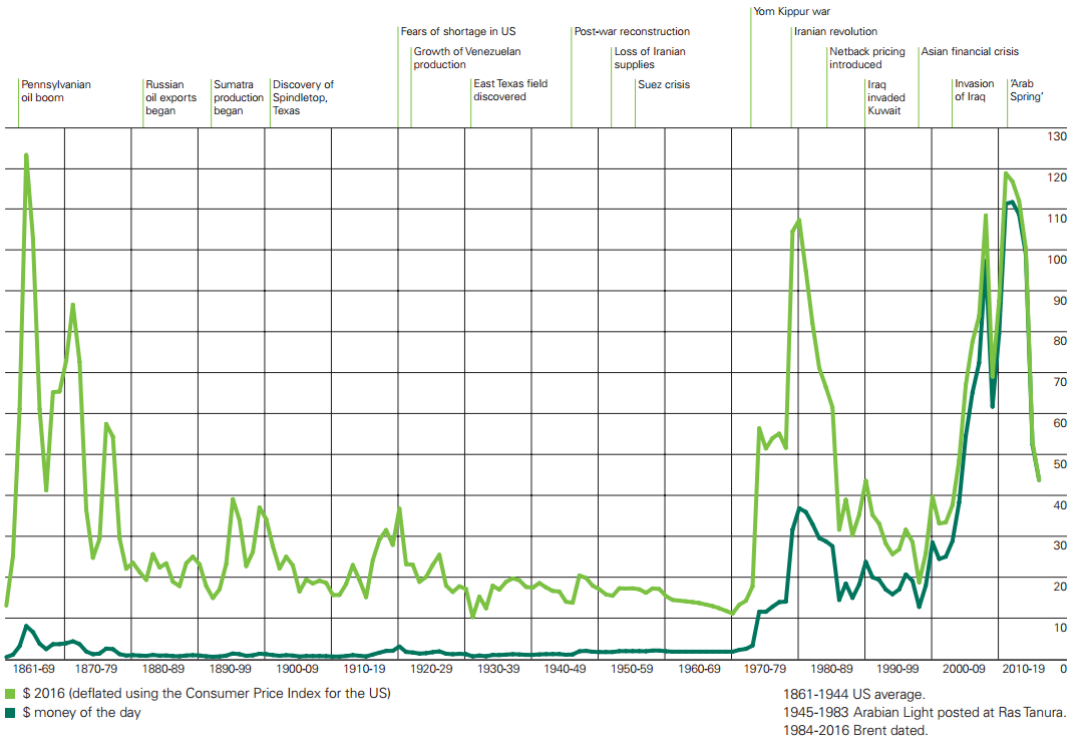

Figure 1.3. Crude oil prices between 1861-2016
(Source: BP 2017)

Investigating the source of CO_2 is the easiest way to understand which sector is responsible for fossil fuel utilization. In European Union countries, 55% of the total CO_2 released to the atmosphere came from the energy sector, while transportation comes second with 23%. (Figure 1.4) Similarly, in Turkey, 62% of the total CO_2 came from energy production while 14% produced from transportation. (Figure 1.5) In order to control air pollution, while also increasing the renewable fuel usage in the transportation sector, European Union implemented policies such as Clean Air Policy Package and Clean Power for Transport policy (EUComm. 2014, EUComm 2013)

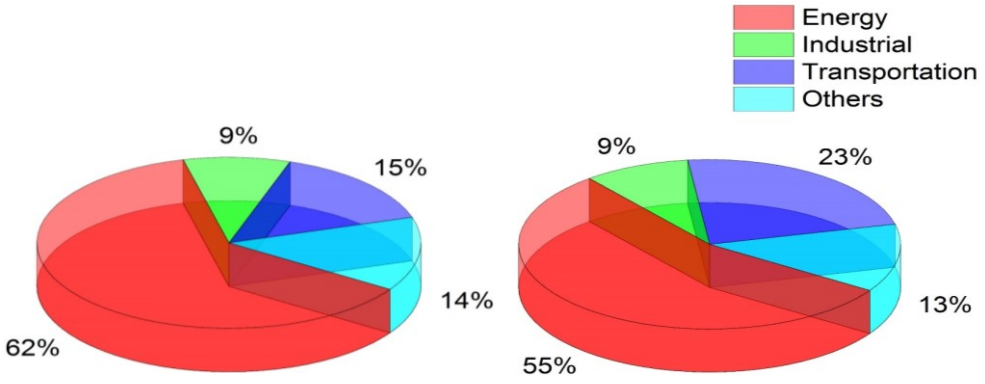

Figure 1.4. Total CO_2 emission in the European Union in 1990 (left) and 2015 (right)
(Source: EEA 2017)

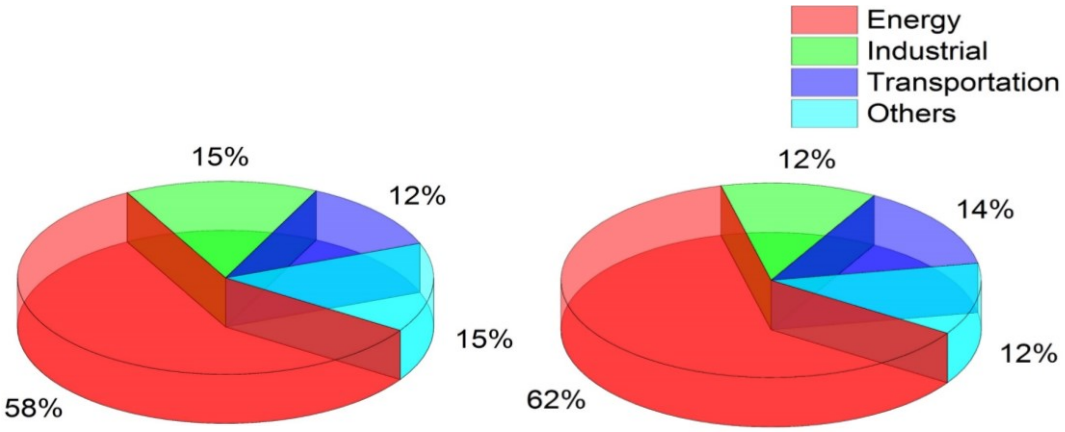

Figure 1.5. Total CO_2 emission in the Turkey in 1990 (left) and 2013 (right) (Source: TurkStat 2015)

Different feedstocks and reaction routes are proposed over the years, shown in Figure 1.6, to produce renewable fuels. Among these feedstocks, vegetable oils are used to produce biodiesel in industrial scale dating back to 1990's. While most rely on vegetable sources, developments enabled the utilization of unusable oils, such as waste oils and animal fats, reducing the cost and environmental effect even further.

As a fuel source, biodiesel has many advantages. In everyday use, biodiesels blended with petroleum diesel reduces the production of diesel particulate matters as well as CO and hydrocarbons in the exhaust gases. Coupled with reduced CO_2 emission from petroleum, its utilization has advantages in environment area. (Bugarski, Hummer, and Vanderslice 2016)

Despite its economic and environmental advantages, utilization of biodiesel possesses some disadvantages regarding technical and chemical differences with regards to petroleum diesel such as;

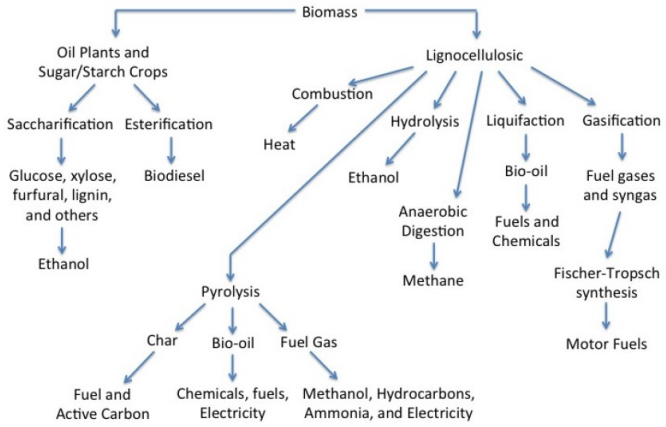

Figure 1.6. Renewable feedstocks and their reaction routes (Source: Dickerson and Soria 2013)

- Lower energy density, amount of energy stored in a specified volume, compared to normal diesel at around 12% due to oxygenated nature of the biodiesel.(Shahid and Jamal 2011)
- Low chemical stability under normal storage conditions as a result of oxidation of the fatty acids when comes contact with air. (Khan and el Dessouky 2009)
- Relatively higher NO_x emission to the atmosphere during combustion, due to oxygenated nature, as well as different combustion characteristics. (Jain and Sharma 2010)
- Public repercussion about the utilization of food resources such as edible oils for the production of biodiesel that would affect the food prices negatively in large-scale production scenarios. (Yusuf, Kamarudin, and Yaakub 2011)
- Higher production costs compared to petroleum-based diesel. (Apostolakou et al. 2009)

Serious as they seem, these problems are just technical difficulties that were encountered during the development of biodiesel. While low chemical stability can be overcome by better logistics and storage conditions, catalytic converters that are mandatory in most countries, with the recent enhancements over their effectiveness, significantly eliminates the NO_x release to the atmosphere. Reducing the amount of oxygen presented in the biodiesel by chemical methods such as hydrothermal treatment can increase the energy density. Negative public perception and higher production costs can be eliminated by utilization of non-edible vegetable oils to both lessen the effect on food industry while also reducing the overall production costs.

Current industrial scale production method follows the transesterification route for biodiesel production. In this method, shown in Figure 1.7, triglyceride inside the oil reacts with an alcohol, in many cases methanol, in the presence of a homogeneous base catalyst, sodium or potassium hydroxide to produce fatty acid methyl esters (FAME's) and glycerol in the process. If the feedstock possesses free fatty acids (FFA's), they are reacted with base catalyst to produce soap. (Figure 1.8)

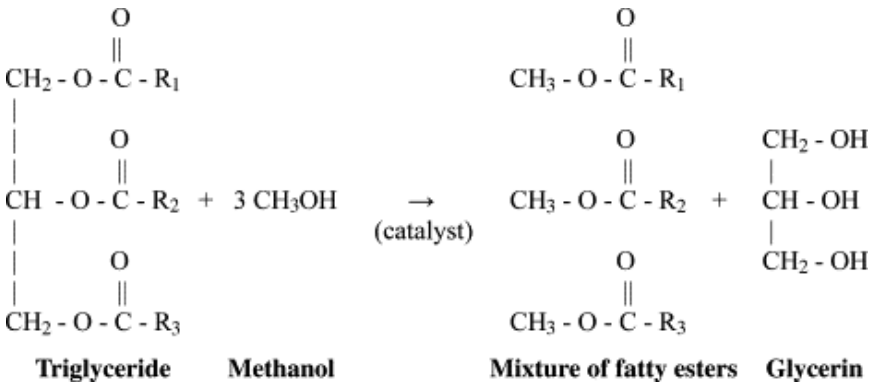

Figure 1.7: Biodiesel transesterification route
(Source: Van Gerpen 2005)

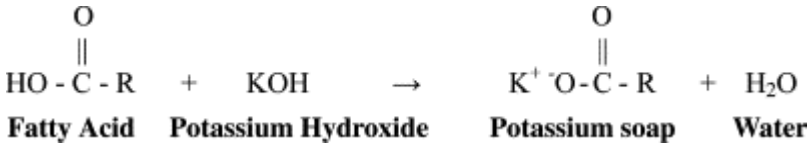

Figure 1.8. FFA soap production
(Source: Van Gerpen 2005)

Production of soap products, as well as the added difficulty and cost of recovery of unreacted base catalyst, have forced researchers to come up with heterogeneous catalysts that could be tailored to reduce soap production while also significantly increasing the recovery rate of catalyst for future use. MgO, CaO, CaO/Al_2O_3, Li-ZnO catalysts are few examples of heterogeneous base catalysts that researchers studied in recent years. (Endalew, Kiros, and Zanzi 2011)

The problem arises with the base catalyst is the unwanted side reaction with FFA's that produces soap-like products. Any FFA in the feedstock would potentially block the active site on the base catalyst, resulting in lower activity towards biodiesel production. That is why researchers increased their attention to the heterogeneous acid catalysts that promote esterification pathway. In esterification, triglyceride reacts with a hydrogen source, pure hydrogen or water, over an acid catalyst to produce glycerol and fatty acid (triglyceride hydrolysis), then fatty acid reacts with alcohol to produce ester products. (Figure 1.9) The advantage of acid catalysts arises when the reaction temperature is elevated to promote deoxygenation reactions such as decarboxylation and decarbonylation, producing higher energy density biodiesel in the process. (Figure 1.10)

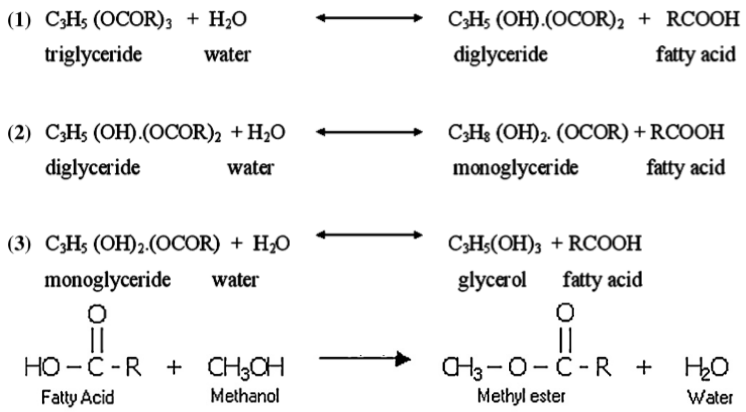

Figure 1.9. Biodiesel esterification route
(Source: Alenezi et al. 2010, Corro et al. 2011)

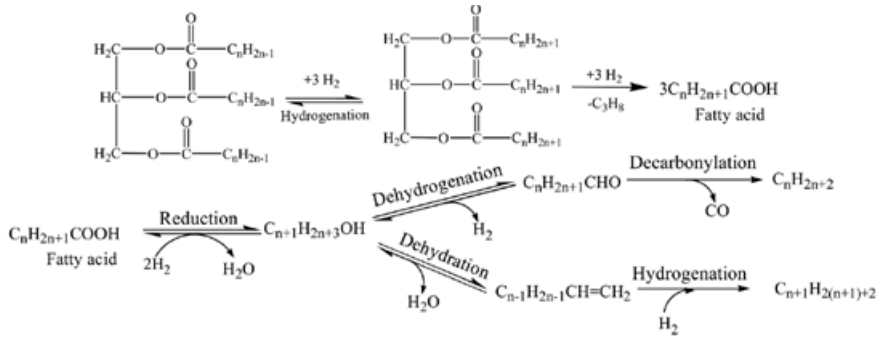

Figure 1.10. Biodiesel deoxygenation route
(Source: Yenumala, Maity, and Shee 2016)

Many of the studies aiming acid catalysts focused on the different zeolites as a catalyst. In zeolite studies, HZSM-5, H-Beta, and H-MOR catalysts gave good conversion values over 70%, however, they performed poorly compared in conversion and reaction time perspective against their base catalyst counterpart. Changing Si/Al ratio of the zeolite catalysts also affected the reaction results as the lowering this ratio increased the acidity and esterification reactions while the opposite is true for basicity and transesterification reactions. (Endalew, Kiros, and Zanzi 2011) They have also investigated the effect of rare earth and transition metals on the biodiesel production since these metals help with deoxygenation as well as hydrogenation of the feedstock. Utilization of rare earth metal such as Pt, Pd and Ru and transition metals such as Co, Mo, and Ni resulted in increased activity. (Hermida, Abdullah, and Mohamed 2015) In many studies, utilization of metals done over the support material; zeolite, alumina or silica, via co-precipitation, wet impregnation or incipient wetness impregnation that come with few drawbacks, such as reduced pore volumes due to blockage, lowered bimetallic interaction between support

and metal. In general, acid catalysts required higher temperatures, up to 130ºC, to achieve better results while eliminating soap byproduct. To increase the energy density and deoxygenation pathways, reaction temperatures up to 300ºC has to be utilized under hydrogen or water presence in the reaction medium.

In this study, canola oil is used as feedstock to convert into biodiesel/hydrocarbons at 115ºC and 1 atm over nickel supported over alumina-silica catalyst prepared with single step sol-gel method. The effect of acidity/acidic strength on conversion of canola oil into useful products as well as selectivity towards esters/hydrocarbons is also investigated. Acidic and textural properties of the catalyst changed with changing Si/Al ratio, Ni ratio, and calcination temperature. Acidic properties also changed with changing the type of acid used in the sol-gel process as HNO_3, H_2SO_4, and H_3PO_4.

CHAPTER 2

LITERATURE SURVEY

2.1. Organic Acid Composition of the Vegetable and Animal Oils

Most of the plan based oils obtained with mechanical or chemical extraction methods from vegetables contain triglyceride based lipids. These triglycerides, with respect to the type of plant they obtained, could possess different chain length fatty acids with varying degree of saturated carbon-carbon bonds in their structure. Common fatty acids observed with vegetable oils can be listed as; palmitic (C16:0), palmitoleic (C16:1), stearic (C18:0), oleic (C18:1), linoleic (C18:2), linolenic (C18:3), arachidic (C20:0), behenic (C22:0), lignoceric (C24:0). Fatty acid types mostly are written in C(XX: Y) form, where XX is the number of carbons in fatty acid and Y is the number of unsaturated carbon-carbon bonds in the fatty acids. Fatty acids containing 20 or more carbons represent only a trace amount of fatty acids in the oil, the bulk of it contains 16 and 18 carbons with varying saturation. (Stedile et al. 2015)

The overall fatty acid composition of feedstock not only changes the final biodiesel ester composition but also changes its chemical properties drastically. Several analysis methods used to determine these properties. Iodine value (IV) of the final biodiesel roughly estimates the biodiesel storage stability. Lower oxidation stability during storage observed with biodiesels having higher IV value because of higher unsaturation of the feedstock. Similar to the octane number of gasoline, cetane number (CN) shows the performance of the biodiesel. Longer chain length with less unsaturation generally gives higher cetane numbers, in some cases higher than petroleum diesel. (Pinzi et al. 2009) Other properties such as flash point, kinematic viscosity, acid number, cold and pour point etc. give a complete picture about the nature of the biodiesel obtained at the end of the process. (Atabani et al. 2013)

Table 2.1. Typical fatty acid composition of various vegetable and animal oils
(Source: Stedile et al. 2015)

Biomass	Unit	Palmitic (C16:0)	Palmitoleic (C16:1)	Stearic (C18:0)	Oleic (C18:1)	Linoleic (C18:2)	Linolenic (C18:3)	Arachidic (C20:0)	Behenic (C22:0)	Lignoceric (C24:0)
Yellow grease	wt%	23	1	10	50	15				
Lard	wt%	25–30	2–5	12–16	41–51	4–22				
Tallow	wt%	25–30	2–3	21–26	39–42	2				
Canola oil	wt%	4		2	60	20	10			
Rubber seed oil	%	8.8		7.7	24	36.1	36.1	Trace		
Poultry	%	22			34	15				
Lamb	%	28		23	32					
Swine	%	16		11	18				10	
Sunflower oil	wt%	6.9		1.9	19.7	71.3				
Safflower seed oil	wt%	7.3		1.9	13.6	77.2				
Jatropha oil	wt%	11.3		17	12.8	47.3		4.7	0.6	44
Rapeseed oil	m%	4.8		1.8	61.8	20.5	7.5			
Soybean oil	m%	11.2		3.1	25.7	53	5.6			
Palm oil	m%	43.7		4.4	39.5	9.77	0.1			
Olive pomace oil	%	10.68	0.7	3.1	74.63	8.68	0.82	0.38	0.2	0.24
Crude palm oil	%	40–45	0.3–0.4	5–6	36–40	9–11	0.2–0.3	0.3–0.4		
Used palm oil	%	22.47	7.56	12.51	27.64	14.58	1.55	0.64		
Waste cooking oil	wt%	24.6	4.5	18.4	46	3.9	0.3	0.9	0.1	
Chicken Fat	%	20	6.2	5.3	39.6	24.7	1.3			

Table 2.1 lists the overall fatty acid composition of different fats and oils that are easily available for biodiesel production. Selection of the correct oil source is important to obtain higher quality product at the end. Using some of the oil alternatives, such as sunflower and jatropha oil for biodiesel production could lower the storage stability of end product because of higher unsaturation. Waste cooking oils are cheap alternatives compared to vegetable oils. However, the cooking process increases the FFA content of the oil. This increase leads to the production of soap-like chemicals during production. In this study, canola oil is chosen as biodiesel feedstock because of its lower unsaturated fatty acid composition and availability.

2.2. Industrial Biofuel Production

Currently, transesterification route is followed in the industrial scale production of biofuel, as biodiesel, all around the world. A simplified version of the process flow chart of the alkali-catalyzed biodiesel production can be seen in Figure 2.1. High FFA content oils first go through a pretreatment process. Homogeneous acid catalysts, such as low concentration of sulfuric acid, in methanol is used to react with FFA via esterification route to obtain esters and water. After neutralization with pretreatment, water should be removed from oil before the transesterification reaction. (Leung, Wu, and Leung 2010) Since using this method comes with problems such as corrosion, catalyst recycle and toxicity, researchers in recent years focused on heterogeneous acidic catalysts for esterification. While it is easy to separate, problems such as low reaction rate and deactivation during reaction inhibit their usage in industrial scale. (Liu et al. 2008)

Before mixing with oil, alkali catalyst, KOH or NaOH, premixed with alcohol, mainly methanol, to produce methoxide solution. The excess catalyst should be added at this point because upon mixing with oil, FFA and alkali catalyst will react with each other to neutralize to the final solution. (Rashid and Anwar 2008) Transesterification reaction will start with alcohol, catalyst, and oil after neutralization. Depending on the scale of the production, continuously stirred reactor (CSTR) or batch reactor is used as reactors. Both pre-heating the oil to higher temperatures and using excess methanol are the proven methods to obtain higher conversions with lower reaction times and readily used in the industry. (Leung and Guo 2006) After the reaction finished, reaction medium contains two main products, esters, and glycerol. Due to density difference, ester and glycerol can be separated easily by phase separation techniques.

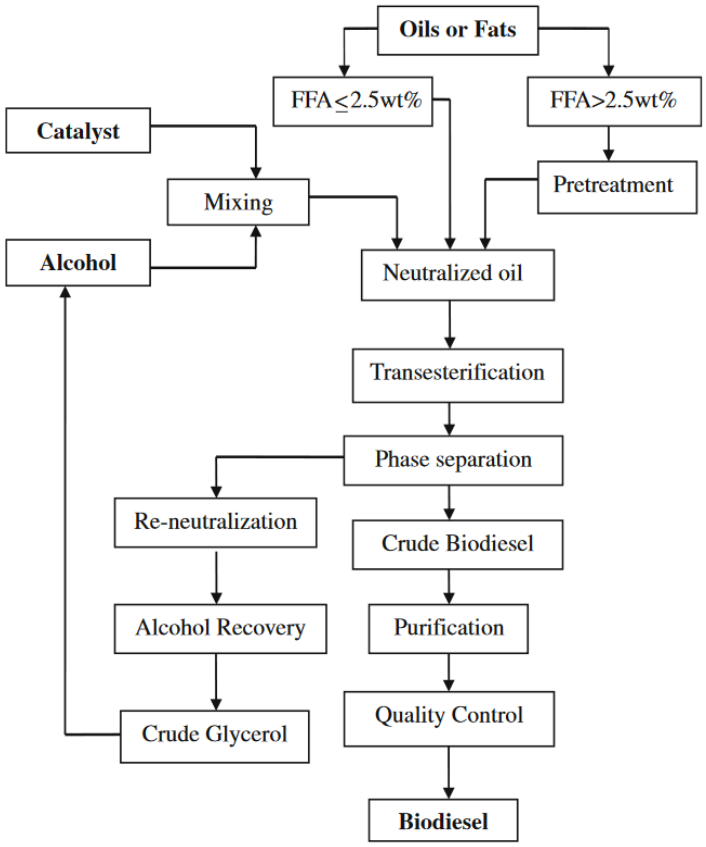

Figure 2.1. Flow diagram of homogeneous alkali catalyzed biodiesel production (Source: Leung, Wu, and Leung 2010)

Main product biodiesel after the separation from glycerol contains esters, unused catalyst, unreacted alcohols, soaps produced from FFA and small amounts of glycerol. To be used in engines it should be purified. Warm water is used in this step since both alcohols and glycerol, as well as soaps, are soluble in water. Addition of small amounts of acids inside washing water also eliminates the unused alkali catalyst. After cleaning, washing water goes to a flash process to recover alcohol for further use. (Van Gerpen et al. 2004)

Although a secondary product, glycerol also has industrial importance and it also goes to the purification process. After separation from biodiesel, it contains glycerol, unreacted alcohol, unused catalyst, and salt. Unused catalyst neutralized by addition of acids, water, and alcohols removed from glycerol by flash processes in liquid form. To be reutilized in transesterification, alcohols further purified to eliminate water going into the reaction. Mostly water and alcohol-free glycerol can be used as crude glycerol or further purified to 99% range for different applications.(Van Gerpen et al. 2004)

Even the above-mentioned process adapted all around the world, using homogeneous alkali catalyst comes with its drawbacks. Soap production during neutralization even with low FFA content, deactivation upon water introduction and their disposable nature can be given as its main problems. To overcome these shortcomings, researchers focus on other alternatives, mainly heterogeneous acidic and alkali catalyst, as well as enzymes. Enzymes, with no soap production with FFA's and better purification of products downstream, are prime candidates for biodiesel production. Due to their low reaction rate and high production costs, they are not available for industrial usage, yet. Current heterogeneous alkali catalyst studies show that using these significantly increase the catalyst's reusability and can be recycled with simple methods for later use. However, they still require water-free operation with higher alcohol-oil ratios and operating temperatures. Heterogeneous acid catalyst comes with a unique property that they can promote both esterification and transesterification reactions due to their different reaction sites. Although they can also be recycled for future use, their low reaction site concentration, coupled with mass transfer problems increases the reaction rate while lowering total biodiesel yield.

2.3. Biofuel Production from Acid Heterogeneous Catalysts

As explained in the previous section, industrial homogeneous base catalysts are easily affected by water, as well as high FFA in the stock oil. To overcome these obstacles, researchers started working on acid catalysts as a possible solution for mentioned problems. Heterogeneous acid catalysts, with their resistance to water and ability to convert FFA without any side products, shifted the focus on this type of catalysts.

If heterogeneous acid catalysts are investigated, it can be said that reactions occur over the acid sites, located on the surface or inside the pores of the catalysts. Depending on how the acidity achieved on these sites, they are categorized as Bronsted and Lewis acid sites. In an aluminosilicate structure, for instance, hydrogen bonded to the oxygen which attaches two cations, aluminum, and silicon, creates Bronsted acid sites, as can be seen in Figure 2.2. Lewis acid sites, contrary to Bronsted sites, observed when an electron imbalance occurs in the aluminosilicate structure, resulting from empty orbital, as can be seen in Figure 2.3. While Bronsted sites donate protons during the reaction, Lewis sites accept electron pairs. (Deka 1998) Depending on the nature of the reaction, Bronsted,

Lewis or combination of both may be necessary for the acid-catalyzed the reaction to occur.

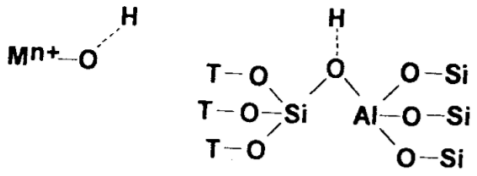

Figure 2.2. Generation of Bronsted acid site over aluminosilicate
(Source: Deka 1998)

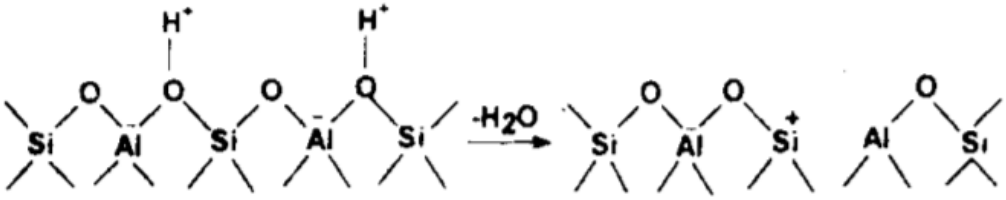

Figure 2.3. Generation of Lewis acid site over aluminosilicate
(Source: Deka 1998)

(1) Decomposition of triglyceride

$CH_2\text{-}OCOR'$ | $CHO\text{-}COCH_2R''$ | $CH_2\text{-}OCOR'''$ → $CHO\text{-}CH{=}CH_2$ (acrolein) + $R'\text{-}COOH$ + $R'''\text{-}COOH$ (fatty acids) + $R''\text{-}CH{=}C{=}O$ (ketenes)

(2) Decomposition of fatty acids

$RCOOH \rightarrow CO_2 + RH$

$2RCOOH \rightarrow CO_2 + H_2O + RCOR$

(3) Decomposition of ketenes and acrolein

$2R''CH{=}C{=}O \rightarrow 2CO + R''HC{=}CHR''$

$CH_2{=}CHCHO \rightarrow CO + C_2H_4$

$RCOCH_2R \rightarrow R\text{–}R + CH_2CO$

$2RCOCH_2R \rightarrow 2R_2 + CO + C_2H_4$

(4) Decomposition into elements

$C_nH_{2n+2} \rightarrow nC + (n+1)H_2$

(5) Dehydrogenation of paraffins

$C_nH_{2n+2} \rightarrow C_nH_{2n} + H_2$

(6) Splitting decomposition of paraffins

$C_nH_{2n+2} \rightarrow C_{n-m}H_{2n-2m+2} + C_mH_{2m}$

(7) Alkylation of paraffins, the reverse of (6)

(8) Isomerization of paraffins

$n\text{-}C_nH_{2n+2} \rightarrow iso\text{-}C_nH_{2n+2}$

(9) Aromatic cyclization of paraffins

$C_{(n+6)}H_{(2n+12)} \rightarrow C_{n+6}H_{2n+6} + 3H_2$

(10) Polymerization of olefins

$2C_nH_{2n} \rightarrow nC_{2n}H_{4n}$

$C_nH_{2n} + C_mH_{2m} \rightarrow mC_{(n+m)}H_{2(n+m)}$

(11) Depolymerization of olefins, reverse of (10)

(12) Decomposition of olefins to diolefins

(13) Decomposition of olefins to acetylenic hydrocarbons

(14) Aromatization or cyclization of olefins

(15) Hydrogenation of olefins

$C_nH_{2n} + H_2 \rightarrow C_nH_{2n+2}$

(16) Isomerization of olefins

$n\text{-}C_nH_{2n} \rightarrow iso\text{-}C_nH_{2n}$

Figure 2.4. Reaction list of triglyceride decomposition
(Source: Xu, Jiang, and Zhao 2016)

Compared to alkali catalyzed reactions, acid catalyzed reactions require higher activation temperatures. Due to this higher temperature, many side reactions could occur during biofuel production. List of possible reactions for triglyceride decomposition with acid catalysts given in Figure 2.4. At the beginning of the reaction, triglycerides that reached to the acid sites decompose into its components, mainly aldehydes (acrolein), fatty acids and, ketenes. With the decomposition, or cracking, of the triglycerides, numerous side reactions can occur depending on the type of acid sites, a number of acid sites and, the reaction conditions. Cracking, hydrogenation, dehydrogenation, deoxygenation, isomerization, polymerization and, aromatization are the side reactions that could be observed during the biofuel production. (Xu, Jiang, and Zhao 2016, Yenumala, Maity, and Shee 2016) While reactions such as deoxygenation and hydrogenation improve the quality of final biofuel mixture by reducing unsaturation and oxygen content, reactions such as aromatization, polymerization, and excessive cracking are unwanted side reactions because they cause coke formation as well as incondensable gas formation. Reduction of unwanted side reactions during biofuel production is one of the main concerns for catalyst selection with product selectivity and yield.

While acidic strength and number of acidic sites, for an acidic heterogeneous catalyst, are important, they alone cannot guarantee a good biofuel yield and/or selectivity on their own. Addition of noble or transition metals on supports such as zeolite and alumina promote the hydrodeoxygenation and hydrodecarboxylation reactions, which in turn decreases the oxygen content and improve the quality of final product. Noble metals such as Palladium (Pd), Ruthenium (Ru) and Platinum (Pt) and, transition metals such as Cobalt (Co), Nickel (Ni), Tungsten (W) and, Molybdenum (Mo) are considered some of the best candidates for the above-mentioned reactions. (Galadima and Muraza 2015) Current studies mostly focus on product selectivity, as well as the effect of reaction conditions and overcoming the problem of catalyst deactivation due to coke formation or sintering of loaded metals over the support material.

Some of the catalysts studied for the biofuel production with their starting oil and reaction conditions are listed in Table 2.2. Most studies listed below focused on the production of hydrocarbons in the diesel range (C_{12}-C_{18}) while at least one study specifically targeted the formation of gasoline range hydrocarbons (C_6-C_{10}) Only the selectivity of targeted biofuel range is listed in Table 2.2.

Table 2.2. Oil conversion and hydrocarbon selectivity in terms of various heterogeneous acid catalysts and reaction conditions.

Catalyst	Stock	Oil/cat. (g/g)	Temp (K)	Time	P (MPa) (Gas Mix)	Conv. (%)	Sel. (Range)	Reference
1% Pt/H-ZSM5	Jatropha	1	543	12 h	6.5 (H_2/N_2)	100	79% (C_{15}-C_{18})	(Murata et al. 2010)
1% Pt/H-ZSM5	Jatropha	10	543	12 h	6.5 (H_2/N_2)	14.2	16% (C_{15}-C_{18})	(Murata et al. 2010)
20% Re-1% Pt/H-ZSM-5	Jatropha	10	543	12 h	6 (H_2/N_2)	80.0	67% (C_{15}-C_{18})	(Murata et al. 2010)
20% Ni/Al_2O_3	Tristearin	3.6	533	6 h	4 (H_2	27	87% (C_{15}-C_{18})	(Loe et al. 2016)
20% Ni/5% Cu/Al_2O_3	Tristearin	3.6	533	6 h	4 (H_2)	97	95% (C_{15}-C_{18})	(Loe et al. 2016)
20% Ni/Al_2O_3	Tristearin	3.6	573	6 h	4 (H_2)	98	97% (C_{15}-C_{18})	(Loe et al. 2016)
20% Ni/5% Cu/Al_2O_3	Tristearin	3.6	573	6 h	4 (H_2)	>99	99% (C_{15}-C_{18})	(Loe et al. 2016)
20% Ni/1% Sn/Al_2O_3	Tristearin	3.6	623	6 h	4 (H_2)	>99	97% (C_{15}-C_{18})	(Loe et al. 2016)
H-ZSM5	Triolein	2.5	723	12 s	Atm.[a]	77.5	40.7% (C_6-C_{110})	(Vu et al. 2015)
H-ZSM5AAT[b]	Triolein	2.5	723	12 s	Atm.[a]	84.6	42.7% (C_6-C_{10})	(Vu et al. 2015)
3.7%Ni/14% Mo/Al_2O_3	WCO[c]	20	623	3 h	7 (H_2)	99.8	94.8% (C_{15}-C_{18})	(Toba et al. 2011)
3.7% Co-14% Mo/Al_2O_3	WCO[c]	20	623	3 h	7 (H_2)	99.6	82.8% (C_{15}-C_{18})	(Toba et al. 2011)
4.2% Ni/29% W/Al_2O_3	WCO[c]	20	623	3 h	7 (H_2)	99.6	96% (C_{15}-C_{18})	(Toba et al. 2011)

(Cont. on next page)

Table 2.2. Cont.

Catalyst	Stock	Oil/cat. (g/g)	Temp (K)	Time	P (MPa) (Gas Mix)	Conv. (%)	Sel. (Range)	Reference
3.7%Ni/14% Mo /B_2O_3-Al_2O_3	WCO[c]	20	623	3 h	7 (H_2)	99.9	91.4 (C_{15}-C_{18})	(Toba et al. 2011)
NiMo/γ-Al_2O_3 (Sulf.[d])	Soybean	22.7	673	2 h	9.2 (H_2)	92.9	97.8% (C_{12}-C_{18})	(Veriansyah et al. 2012)
5% Pd/γ-Al_2O_3	Soybean	22.7	673	2 h	9.2 (H_2)	91.9	93.5% (C_{12}-C_{18})	(Veriansyah et al. 2012)
3.5% Co-14% Mo /γ-Al_2O_3 (Sulf.[d])	Soybean	22.7	673	2 h	9.2 (H_2)	78.9	82.3 (C_{12}-C_{18})	(Veriansyah et al. 2012)
66.0% Ni/(SiO_2-Al_2O_3)	Soybean	22.7	673	2 h	9.2 (H_2)	60.8	95% (C_{12}-C_{18})	(Veriansyah et al. 2012)
5% Pt/Al_2O_3	Soybean	22.7	673	2 h	9.2 (H_2)	50.8	96% (C_{12}-C_{18})	(Veriansyah et al. 2012)
5% Ru/Al_2O_3	Soybean	22.7	673	2 h	9.2 (H_2)	39.7	99% (C_{12}-C_{18})	(Veriansyah et al. 2012)

[a]: Atmospheric pressure [b]: Alkaline-Acid treatment [c]: Waste cooking oil [d]: Sulfided catalyst

Noble metal loading over zeolites and alumina supports were one of the most studied catalysts due to their high activity. Even a 1% Pt loading on H-ZSM5 catalyst at relatively low oil/catalyst ratios gave very high oil conversion as well as comparatively high selectivity towards hydrocarbons in the range of C_{15}-C_{18}. (Murata et al. 2010) However, increasing the oil/catalyst ratio to 10 significantly decreases the conversion and selectivity because, at this oil/catalyst ratio, the catalyst can only hydrogenate the unsaturated structures. To eliminate this problem, Rhenium (Re) added to the Pt-loaded catalyst to obtain 20% Re-1% Pt/H-ZSM-5 catalyst. Using this catalyst, even at high oil/catalyst ratio resulted in very high conversion and selectivity. Thus, the addition of Re on Pt catalyst had a synergetic effect which increased the effectiveness of the catalyst by promoting decarboxylation and hydrodeoxygenation on Re while support H-ZSM5 acted as a hydrocracking catalyst.

In another study performance of both noble and transition metals as well as sulfided bimetallic catalysts were investigated. For the given reaction conditions, sulfided NiMo/γ-Al_2O_3 gave the best conversion and selectivity while 5% Ru/Al_2O_3 performed poorly.(Veriansyah et al. 2012) Compared to the previous study, a decrease in the acidic strength of the support material resulted in high diesel range selectivity with low light olefin yield for Pd, NiMo, Ni and Pt catalysts. On the other hand, CoMo catalyst resulted with higher naphtha selectivity and lower diesel selectivity because of its higher hydrocracking potential, Since Ru catalyst is an outstanding methanation catalyst, this explains the low conversion of large triglycerides typically found in vegetable oils.

The composition of the support material has also significant outcomes on the biofuel production. Using Al_2O_3 as support material, production of diesel range hydrocarbons from waste cooking oil (WCO) using sulfided NiMo, CoMo and NiW catalysts showed that best performing catalyst for diesel range hydrocarbons was NiMo/Al_2O_3.When Boron Trioxide (B_2O_3) added to support material to obtain B_2O_3-Al_2O_3, selectivity towards isomerization reactions doubled with the increase in the acidity of support, from 3.8% to 7.5%, compared to NiMo/Al_2O_3 catalyst under the same condition. (Toba et al. 2011) As a result of using sulfided catalyst, sulfur release to the product observed during the first 24 h of reaction. Initial sulfur release results with a decrease in n-paraffin formation for all catalyst and stabilizes after 5 h except for CoMo/B_2O_3-Al_2O_3 catalyst. Loss of sulfur resulted with deactivation of hydrogenation

active sites for $CoMo/B_2O_3$-Al_2O_3 catalyst, thus rendering it ineffective at the given reaction conditions. Investigations showed that NiMo catalyst promoted the hydrogenation-dehydration route while NiW catalyst promoted decarboxylation-decarbonylation pathways for diesel-range hydrocarbon formation.

Besides the studies focusing on existing commercial catalysts such as NiMo, CoMo, Pt and, Pd supported on Al_2O_3, researchers also look into different transition metal catalyst supported alumina. One of the area for consideration is the bimetallic interaction between different transition metals onto each other and it was investigated over 20% Ni/Al_2O_3 catalyst by incorporating Copper (Cu) and Tin (Sn). (Loe et al. 2016) Studies done for the conversion of triolein at 533 K showed that addition of Cu to produce 20% Ni/5% Cu/Al_2O_3 catalyst significantly increased the conversion and selectivity towards diesel-range products compared to 20% Ni/Al_2O_3 while effect of Sn addition was not observed until reaction temperature increased to 623 K. Analysis on 20% Ni/Al_2O_3 and 20% Ni/5% Cu/Al_2O_3 catalysts showed that presence of 5% Cu on catalyst both increased the reducibility of Ni while preventing excessive cracking and coke formation, which increases the catalytic activity and deactivation, respectively.

From the experience gained in the petroleum industry, zeolite catalysts are very good candidates for the biofuel production because of their cracking potential. (Satterfield 1991) While having excellent micropore structure with high acidity, limitations due to the small pore size of zeolites resulted in excessive cracking and coke formation, eventually deactivating the catalyst. To overcome these shortcomings, modification on the H-ZSM5 catalyst with various methods such as back to back alkaline and acid treatment investigated by researchers. (Vu et al. 2015) It was observed that, at the same reaction conditions, compared to the unmodified H-ZSM5 catalyst, higher conversion and selectivity was achieved with alkaline-acid treated H-ZSM5. Increasing the external surface area coupled with a decrease in the micropore diffusion path length after alkaline-acid treatment resulted in conversion increase and a decrease in excessive cracking, respectively.

Despite all the studies done on this current subject, very few studies focused on the low-temperature conversion of vegetable oils. Additionally, most of the metal loaded catalysts, both commercial and laboratory made, use impregnation method for catalyst preparation. Using this method while easier has few shortcomings, such as localization

of the metal-support interaction and, the possibility of pore mouth blockage from metal loading, which needs to be addressed for large-scale applications. The single step sol-gel method overcomes these problems by incorporating the metal loading into support structure thus increasing the metal-support interaction and preventing pore blockage. In this study, low-temperature biofuel production from canola oil investigated by using Ni loaded Al_2O_3-SiO_2 heterogeneous acid catalysts. Different acids, HNO_3, H_2SO_4 and, H_3PO_4 will be used during the single step sol-gel catalyst preparation to observe the change in the physical and chemical properties of the support material.

CHAPTER 3

MATERIALS AND METHODS

3.1. Materials

Ni/Al_2O_3-SiO_2 catalysts with varying nickel and Al/Si ratios were synthesized using single step sol-gel method. catalyst surface, as well as its chemical structure. Nickel(II) acetate hydrate was used as nickel precursor while aluminum isopropoxide (AIP) and tetraethyl orthosilicate (TEOS) were used as alumina and silica precursors, respectively. During catalyst preparation, ethanol (EtOH) and deionized water (DIW) used as solvents while n-hexane used for GC-MS analysis. Hydrochloric acid (HCl) was used as peptization agent for silica preparation while nitric acid (HNO_3), sulfuric acid (H_2SO_4) and phosphoric acid (H_3PO_4) used in the same manner for alumina preparation. Detailed list of the chemicals used in the catalyst preparation listed in Table 3.1.

Table 3.1. List of chemicals used in the synthesis of catalysts and their properties

Chemical Name	Chemical Formula	Molecular Weight (g/mol)	Density (g/cm^3)	Purity (%)
Aluminum Isopropoxide	$Al(C_3H_7O)_3$	204.24	1.035	98
Tetraethyl Orthosilicate	$Si(C_2H_5O)_4$	208.33	0.934	99.9
Hydrochloric Acid	HCl	36.45	1.17	37
Nitric Acid	HNO_3	63.01	1.4	65
Sulfuric Acid	H_2SO_4	98.08	1.84	96
Phosphoric Acid	H_3PO_4	98	1.685	85
Nickel(II) Acetate Hydrate	$Ni(CH_3COO)_2.H_2O$	176.79	---	99
Ethanol	C_2H_5OH	46.07	0.79	99.5
Water	H_2O	18.02	0.999	1
n-Hexane	C_6H_{14}	86.18	0.659	99

Commercial canola oil () and Ni/Al_2O_3-SiO_2 catalysts were used to carry out the heterogeneous biofuel production reactions.

3.2. Catalyst Preparation

To synthesize Ni on Al_2O_3-SiO_2 catalyst, Al_2O_3 precursor was prepared using a modified single step sol-gel method. (Yoldas 1975) To prepare the alumina part of the catalyst, aluminum isopropoxide (AIP) added to the water at 85°C and mixed for 1 hour. After mixing, depending on the type of the catalyst that was wanted to make, required amounts of nitric acid (HNO_3), sulfuric acid (H_2SO_4) or phosphoric acid (H_3PO_4) added to this solution and mixed for another 1 hour.

Silica part of the catalyst also prepared with the sol-gel method. To prepare it, necessary amounts of water, ethanol, tetraethyl orthosilicate (TEOS) and 1 M HCl solution added to a beaker in this order and heated to 80°C for 2 hours.

When both alumina and silica solutions are ready, Nickel(II) acetate hydrate and silica solutions added to the alumina solution and mixed at 85°C. After gelation occurs, Ni/ Al_2O_3-SiO_2 gel dried at 120°C overnight. This catalyst was then calcined, depending on the requirement, between 500 °C to 900 °C for 6 hours with a heating rate of 10 °C/min. To prepare them reaction and analysis ready, calcined catalysts were ground and sieved to obtain particles smaller than 200 mesh (75 μm)

3.3. Biofuel Production with Ni/Al_2O_3-SiO_2 Catalysts

During the study, biofuel production over heterogeneous catalyst carried out with commercial canola oil at 115°C with catalyst/oil ratio of 0.1 (g/g). In a typical experiment, 2 g of canola oil weighed with the analytical balance, then heated to reaction temperature under constant stirring. When the oil reached the reaction temperature, 0.2 g of the catalyst added on top of the oil and reaction carried out for 6 hours at stirring speed of 750 rpm. For product analysis, catalyst and final product separated with centrifuge operating at 25°C with 10,000 rpm for 5 minutes. Liquid and solid part separated and liquid part sent to analysis. Product distribution of the liquid sample diluted with n-hexane and analyzed with gas chromatography-mass spectroscopy (GC-MS, Agilent 6890N with 5973N GC/MSD) equipped with HP-5MS column having the dimensions 0.25 mm * 30 m * 0.25 μm. NIST MS database is used to characterize the chromatogram peaks.

3.4. Box Behnken Design for Catalyst Composition Selection

In normal circumstances, in order to understand the relationship between a variable and its effect on the experiment, multiple experiments must be run while changing variables and follow the results by hand. However, doing this comparison by hand for more than 3 variable becomes cumbersome while also time inefficient. A better way to conduct this analysis is to construct an experimental design which computes the relationship between multiple variables and their effects on the experimental results statistically. With this approach, an empirical model which is first or higher order polynomial equation fitted to the experimental results, called response, to show the effect of individual factors and/or interaction between the factors. (Montgomery 2014)

$$y_i = \beta_0 + \beta_1 x_{i1} + \cdots \beta_k x_{ik} + \beta_{11} x_{i1}^2 + \cdots + \beta_{kk} x_{ik}^2 + \beta_{12} x_{i1} x_{i2} + \cdots + \beta_{k-1,k} x_{i,k-1} x_{ik} \quad (3.1)$$

During the study, experimental design variables set as Aluminum concentration (A), Nickel concentration (B), calcination temperature (C) and acid type of the catalyst used in the experiment while responses determined as final product composition in 4 main product types, aldehydes, esters, organic acids and others which contains products such as alcohols, furans, ketones etc. Optimization of catalyst compositions using the results done by response surface methodology method. Box Behnken design used with three continuous factors (A, B and C) having two levels and one categorical design (D) with three levels. With three center point experiments as repetition, the total number of reactions found to be 15 for each acid type. Final catalyst compositions and catalyst names are given in Table 3.2, Table 3.3 and Table 3.4 for the catalysts prepared with HNO_3, H_2SO_4, and H_3PO_4, respectively.

3.5. Catalyst Characterization

Catalyst crystal structures were determined by X-Ray Diffraction with Philips X'Pert Pro Diffractometer using Ni/filtered CuK_a radiation (λ=1.54056 Å) in the range of 5-80^o 2θ values. Crystalline size of the catalysts was determined from XRD spectra using Debye-Scherrer Equation (3.2).

$$C = \frac{K * \lambda}{B * \cos(\Theta)}$$

(3.2)

where C is crystal size, K is Scherrer shape factor, which is generally taken as 0.94 assuming sphere crystals and B describes the full width at the half maximum intensity (FWHM) of the peak in terms of radians.

Analysis of the surface area and pore structure done by Brunauer, Emmet and Teller (BET) method using N_2 adsorption isotherms obtained at 77 K using Micromeritics Gemini V volumetric adsorption device. Before adsorption of N_2, samples degassed at 300ºC under vacuum (10^{-6} Torr) for 24 h. Results from BET analysis will be used to determine the catalyst topology via adsorption isotherm. (Thomas and Thomas 2014)

Investigation of the acidity and acid strength of the solid catalyst done by adsorbing a basic gas, such as NH_3, using temperature programmed desorption (TPD) device. (Micromeritics AutoChem 2920) Prior to NH_3 adsorption, similar to BET procedure, sample heated to 800ºC under helium flow to eliminate any adsorbed species from the catalyst surface.

Table 3.2. Names and composition of catalysts prepared with HNO3

Code	Al Content (%)	Ni Content (%)	Calc. Temperature (ºC)
A-01	25	0	700
A-02	75	0	700
A-03	25	20	700
A-04	75	20	700
A-05	25	10	500
A-06	75	10	500
A-07	25	10	900
A-08	75	10	900
A-09	50	0	500
A-10	50	20	500
A-11	50	0	900
A-12	50	20	900
A-13	50	10	700

Table 3.3. Names and composition of catalysts prepared with H2SO4

Code	Al Content (%)	Ni Content (%)	Calc. Temperature (ºC)
B-01	25	0	700
B-02	75	0	700
B-03	25	20	700
B-04	75	20	700
B-05	25	10	500
B-06	75	10	500
B-07	25	10	900
B-08	75	10	900
B-09	50	0	500
B-10	50	20	500
B-11	50	0	900
B-12	50	20	900
B-13	50	10	700

Table 3.4. Names and composition of catalysts prepared with H_3PO_4

Code	Al Content (%)	Ni Content (%)	Calc. Temperature (ºC)
C-01	25	0	700
C-02	75	0	700
C-03	25	20	700
C-04	75	20	700
C-05	25	10	500
C-06	75	10	500
C-07	25	10	900
C-08	75	10	900
C-09	50	0	500
C-10	50	20	500
C-11	50	0	900
C-12	50	20	900
C-13	50	10	700

Table 3.5. List of continuous and categorical factors used in the experimental design

	Continuous Factor			Categorical Factor
Level	Al Content (%)	Ni Content (%)	Calc. Temperature (°C)	Acid Type
Low	25	0	500	HNO_3
Center	50	10	700	H_2SO_4
High	75	20	900	H_3PO_4

CHAPTER 4

RESULTS AND DISCUSSION

Biofuel production over Ni supported on Al_2O_3-SiO_2 catalysts with different acids as peptization agent was studied in a glass reactor. Liquid products were analyzed with GC-MS and aldehydes, esters, organic acids, and other compounds yield calculated from total GC-MS chromatogram area. List of the compounds detected with GC-MS with their type and retention times given in Appendix A.1. Calculated aldehyde, ester, organic acid and other compound yields for catalysts prepared with HNO_3, H_2SO_4 and H_3PO_4 acids listed in Table 4.1, Table 4.2 and Table 4.3, respectively.

4.1. Analysis of Variance Studies for Aldehydes, Esters, Organic Acids and Other Compound Yields

In order to come up with an empirical model that can explain the individual and/or coupled effect of each variable, ANOVA test was conducted for each product type with confidence interval value set to 90%. Table 4.4 gives the ANOVA analysis results done on ester yield. P-value is the key to investigating which parameters are affecting the response. Parameters that have low p-values ($p<0.1$) show there is a strong interaction between parameter and response, thus included in the model. Parameters having higher p-values are excluded from empirical model since the interaction between these factors and response are not significant enough to put into the model and their effect calculated as Error, shown in Table 4.4. As it can be seen, aluminum and nickel concentration on their own have p-values of 0.664 and 0.703 respectively, which makes them insignificant according to the above rule. However, their two-way interactions, Al Cont.*Ni Cont. and Ni Cont.*Calc. Temp both have p-values lower than 0.1. Since their coupled interactions are significant in the model equation, their individual effect, no matter how small they are, included in the model. Coupled effect from Al Cont.*Ni Cont. comes from the bimetallic interaction between aluminum and nickel while Ni Cont.*Calc. Temp comes from different nickel phases with temperature change.

Table 4.1. Box Behnken design and responses as aldehydes, esters, organic acids and others for the catalysts prepared with HNO_3

Code	Factor	Al Content (%)	Ni Content (%)	Calcination Temperature (°C)	Aldehyde (%)	Ester (%)	Org. Acid (%)	Other (%)
A-01	--0	25	0	700	11.43	32.51	45.99	10.07
A-02	+-0	75	0	700	4.18	30.34	59.52	5.96
A-03	-+0	25	20	700	0.19	32.22	63.38	4.22
A-04	++0	75	20	700	4.57	27.68	59.44	8.31
A-05	-0-	25	10	500	19.44	22.08	47.80	10.68
A-06	+0-	75	10	500	5.38	29.87	54.60	10.15
A-07	-0+	25	10	900	3.07	36.45	54.60	5.89
A-08	+0+	75	10	900	3.80	28.58	54.50	13.12
A-09	0--	50	0	500	2.95	40.02	51.79	5.23
A-10	0+-	50	20	500	5.28	30.27	51.77	12.68
A-11	0-+	50	0	900	1.63	33.66	50.17	14.54
A-12	0++	50	20	900	18.05	29.85	47.59	4.52
A-13	000	50	10	700	3.99	32.66	50.01	13.35
A-14	000	50	10	700	4.35	33.64	54.72	7.29
A-15	000	50	10	700	3.79	32.31	56.67	7.23

(+) High
(0) Center
(-) Low values for design variables

Table 4.2. Box Behnken design and responses as aldehydes, esters, organic acids and others for the catalysts prepared with H_2SO_4

Code	Factor	Al Content (%)	Ni Content (%)	Calcination Temperature (°C)	Aldehyde (%)	Ester (%)	Org. Acid (%)	Other (%)
B-01	--0	25	0	700	1.05	26.56	66.25	6.01
B-02	+-0	75	0	700	14.55	29.34	47.73	8.37
B-03	-+0	25	20	700	8.85	32.84	45.78	12.53
B-04	++0	75	20	700	8.20	33.91	47.51	10.38
B-05	-0-	25	10	500	18.34	34.77	33.83	13.06
B-06	+0-	75	10	500	9.12	26.17	56.45	8.26
B-07	-0+	25	10	900	6.78	30.74	54.61	7.87
B-08	+0+	75	10	900	3.34	23.39	65.89	7.38
B-09	0--	50	0	500	15.09	24.74	49.65	10.52
B-10	0+-	50	20	500	1.90	33.78	61.20	3.04
B-11	0-+	50	0	900	3.10	27.14	60.12	9.64
B-12	0++	50	20	900	3.07	21.70	66.86	6.99
B-13	000	50	10	700	8.20	22.23	63.14	6.43
B-14	000	50	10	700	7.39	31.54	53.00	8.06
B-15	000	50	10	700	9.98	28.71	54.83	6.48

(+) High
(0) Center
(-) Low values for design variables

Table 4.3. Box Behnken design and responses as aldehydes, esters, organic acids and others for the catalysts prepared with H_3PO_4

Code	Factor	Al Content (%)	Ni Content (%)	Calcination Temperature (°C)	Aldehyde (%)	Ester (%)	Org. Acid (%)	Other (%)
C-01	--0	25	0	700	30.78	14.08	45.37	9.77
C-02	+-0	75	0	700	8.47	11.43	68.60	11.50
C-03	-+0	25	20	700	3.27	10.22	80.43	5.29
C-04	++0	75	20	700	25.36	15.90	50.57	8.17
C-05	-0-	25	10	500	2.07	19.99	74.59	3.34
C-06	+0-	75	10	500	1.92	14.41	76.86	6.16
C-07	-0+	25	10	900	16.76	41.41	34.88	6.96
C-08	+0+	75	10	900	20.73	16.45	55.10	7.72
C-09	0--	50	0	500	3.35	11.87	77.64	6.06
C-10	0+-	50	20	500	1.76	10.94	75.45	11.03
C-11	0-+	50	0	900	24.04	16.08	45.02	14.85
C-12	0++	50	20	900	29.23	16.03	46.60	8.14
C-13	000	50	10	700	19.66	15.29	57.49	7.57
C-14	000	50	10	700	16.51	15.83	61.67	5.99
C-15	000	50	10	700	19.66	15.38	57.84	7.11

(+) High
(0) Center
(-) Low values for design variables

Table 4.4. Calculated ANOVA analysis for aldehyde yield in the product with two-sided 90% confidence interval

Source	DF	Adj SS	Adj MS	F-Value	P-Value
Model	9	0.184	0.020	6.090	0.000
Linear	5	0.075	0.015	4.460	0.003
Al Cont.	1	0.001	0.001	0.190	0.664
Ni Cont.	1	0.000	0.000	0.150	0.703
Calc. Temp.	1	0.009	0.009	2.750	0.106
Acid Type	2	0.064	0.032	9.610	0.000
2-Way Interaction	4	0.109	0.027	8.130	0.000
Al Cont.*Ni Cont.	1	0.015	0.015	4.370	0.044
Ni Cont.*Calc. Temp.	1	0.010	0.010	2.880	0.098
Calc. Temp.*Acid Type	2	0.085	0.042	12.630	0.000
Error	35	0.117	0.003		
Lack-of-Fit	29	0.116	0.004	23.350	0.000
Pure Error	6	0.001	0.000		
Total	44	0.301			

After ANOVA analysis completed and relevant factors including aluminum and nickel concentration, calcination temperature, acid type and their interactions selected, T-values of each included factor shown in Figure C.1, is used to come up with constants of empirical equation proposed in Eqn. 3.1 for each acid type. Eqn. 4.1, Eqn. 4.2 and Eqn. 4.3 gives the aldehyde yield model equations for HNO_3, H_2SO_4, and H_3PO_4 acids, respectively. With R^2 and R^2(adjusted) values around 61% and 51%, shown in Table C.5, it can be said that model is a good approximation for the intended response. Random distribution, as well as disturbance in the results, were also analyzed with histograms and residual analysis of the model, shown in Figure B.1 in Appendix B. Presence of no outliers (extreme results) shown in Figure B.1a means ANOVA analysis is acceptable while Figure B.1b, Figure B.1c, and Figure B.1d shows that there were no patterns in the residual distribution. This is very important because observing a pattern, regular shapes in residual distribution, mean that there is outside factor(s) such as faulty reaction and analysis equipment or human error that alters the response. Since their effect cannot be included in the model, accuracy of model decreases significantly.

$$\text{Aldehydes with } HNO_3 = 0.386 - 0.001603\ A - 0.01736\ B - 0.000318\ C + 0.000140\ A\ *B + 0.000014\ B*C \quad (4.1)$$

$$\text{Aldehydes with } H_2SO_4 = -0.024 - 0.001603\ A - 0.01736\ B + 0.000369\ C + 0.000140\ A*B + 0.000014\ B*C \quad (4.2)$$

$$\text{Aldehydes with } H_3PO_4 = 0.274 - 0.001603\ A - 0.01736\ B - 0.000182\ C + 0.000140\ A*B + 0.000014\ B*C \quad (4.3)$$

ANOVA summary of ester yield given in Table 4.5. As it can be seen, most significant factors are aluminum concentration, acid type, Al Cont.*Calc. Temp. and Calc. Temp.*Acid Type and they are included in the model. While on their own nickel concentration and calcination temperature are not significant, because of their two-way interactions, they too included in the model. Both two-way interactions, Al Cont.*Calc. Temp. and Calc. Temp.*Acid Type comes from different crystal phases generated with different calcination conditions while using different aluminum ratio as well as acid types during catalyst preparation. T-values given in Figure C.2 is used to construct proposed model equations for ester yield which are given in the Eqn. 4.4, Eqn. 4.5 and Eqn. 4.6. Higher R^2 values for models, given in Table C.5, compared to aldehyde yield indicates proposed models are better suited for ester yield analysis. Looking at the histograms and residual plots in Figure B.2 shows that our ANOVA analysis was also acceptable for ester yield with no patterns observed with histograms and residual distribution.

$$\text{Esters with } HNO_3 = 0.200 + 0.00317\ A - 0.00010\ B + 0.000178\ C - 0.000006\ A*C \quad (4.4)$$

$$\text{Esters with } H_2SO_4 = -0.137 + 0.00317\ A - 0.00010\ B + 0.000486\ C - 0.000006\ A*C \quad (4.5)$$

$$\text{Esters with } H_3PO_4 = 0.130 + 0.00317\ A - 0.00010\ B + 0.000321\ C - 0.000006\ A*C \quad (4.6)$$

Table 4.5. Calculated ANOVA analysis for ester yield in the product with two-sided 90% confidence interval

Source	DF	Adj SS	Adj MS	F-Value	P-Value
Model	8	0.228	0.029	11.380	0.000
Linear	5	0.204	0.041	16.240	0.000
Al Cont.	1	0.009	0.009	3.580	0.067
Ni Cont.	1	0.000	0.000	0.010	0.921
Calc. Temp.	1	0.002	0.002	0.840	0.364
Acid Type	2	0.193	0.096	38.380	0.000
2-Way Interaction	3	0.025	0.008	3.280	0.032
Al Cont.*Calc. Temp.	1	0.010	0.010	3.790	0.059
Calc. Temp.*Acid Type	2	0.015	0.008	3.030	0.061
Error	36	0.090	0.003		
Lack-of-Fit	30	0.086	0.003	3.670	0.055
Pure Error	6	0.005	0.001		
Total	44	0.319			

Results of the ANOVA analysis on organic acid yield can be seen in Table 4.6. Calcination temperature, acid type, Al Cont.*Ni Cont. and Calc. Temp.*Acid Type interactions have a significant effect on the organic acid yield. Effect of interaction between aluminum and nickel concentration can be explained with bimetallic interactions while the interaction between calcination temperature and acid type is the result of different crystal phase formation. As of before, effects with high p-values did not include in the system while aluminum and nickel concentration effects were not eliminated from the model since their two-way interactions have a significant effect on the response. From the T-values calculated after ANOVA analysis, given in Table C.3, proposed model equations obtained and are given in Eqn. 4.7, Eqn. 4.8 and Eqn. 4.9. Acceptable R^2 values coupled with histogram and residual analysis given in Figure B.3 indicates that the application of model equations for prediction as well as ANOVA analysis are acceptable.

$$\text{Organic Acids with } HNO_3 = 0.212 + 0.00250\ A + 0.00958\ B + 0.000290\ C - 0.000168\ A*B \tag{4.7}$$

$$\text{Organic Acids with } H_2SO_4 = 1.006 + 0.00250\ A + 0.00958\ B - 0.000768\ C - 0.000168\ A*B \tag{4.8}$$

$$\text{Organic Acids with } H_3PO_4 = 0.394 + 0.00250\ A + 0.00958\ B + 0.000006\ C - 0.000168\ A*B \quad (4.9)$$

Table 4.6. Calculated ANOVA analysis for organic acid yield in the product with two-sided 90% confidence interval

Source	DF	Adj SS	Adj MS	F-Value	P-Value
Model	8	0.291	0.036	6.770	0.000
Linear	5	0.078	0.016	2.910	0.026
Al Cont.	1	0.010	0.010	1.880	0.179
Ni Cont.	1	0.003	0.003	0.640	0.429
Calc. Temp.	1	0.024	0.024	4.440	0.042
Acid Type	2	0.041	0.020	3.790	0.032
2-Way Interaction	3	0.213	0.071	13.200	0.000
Al Cont.*Ni Cont.	1	0.021	0.021	3.920	0.055
Calc. Temp.*Acid Type	2	0.192	0.096	17.850	0.000
Error	36	0.194	0.005		
Lack-of-Fit	30	0.184	0.006	3.980	0.045
Pure Error	6	0.009	0.002		
Total	44	0.485			

ANOVA analysis of other product yields listed in Table 4.7. Unlike previous analyses did on aldehydes, esters, and organic acids, Ni Cont.*Calc. Temp. was the only significant factor that impacted on the other product yield. Other factors including individual and coupled ones had little to no effect on the response. During the study, products such as alcohols, furans, ketones and other hydrocarbons detected with GC-MS collected under the other products category as their individual presence was very low while in some reaction studies, one or more product types were non-existent in the product altogether. Since the other product category affected by multiple factors, lack of significant factors from ANOVA analysis is understandable. Proposed model equations for other product yields using the T-values given in Table C.4 are shown in Eqn. 4.10, Eqn. 4.11 and Eqn. 4.12. Although the histogram and residual analysis in Figure B.4 have shown the ANOVA analysis is acceptable, R^2 values given in Table C.5 indicates that any prediction done by proposed model equations have high uncertainty. Because of this high uncertainty, the other product yield would not be used for optimization studies.

Table 4.7. Calculated ANOVA analysis for other compound yield in the product with two-sided 90% confidence interval

Source	DF	Adj SS	Adj MS	F-Value	P-Value
Model	7	0.008	0.001	1.460	0.213
Linear	5	0.002	0.000	0.610	0.690
Al Cont.	1	0.000	0.000	0.490	0.486
Ni Cont.	1	0.001	0.001	1.530	0.224
Calc. Temp.	1	0.000	0.000	0.280	0.600
Acid Type	2	0.001	0.000	0.380	0.684
2-Way Interaction	2	0.006	0.003	3.560	0.038
Al Cont.*Calc. Temp.	1	0.001	0.001	1.030	0.316
Ni Cont.*Calc. Temp.	1	0.005	0.005	6.090	0.018
Error	37	0.030	0.001		
Lack-of-Fit	31	0.027	0.001	1.900	0.217
Pure Error	6	0.003	0.000		
Total	44	0.038			

$$\text{Others with } HNO_3 = 0.0591 - 0.00101\ A + 0.00638\ B + 0.000033\ C + 0.000002\ A*C - 0.000010\ B*C \quad (4.10)$$

$$\text{Others with } H_2SO_4 = 0.0555 - 0.00101\ A + 0.00638\ B + 0.000033\ C + 0.000002\ A*C - 0.000010\ B*C \quad (4.11)$$

$$\text{Others with } H_3PO_4 = 0.0591 - 0.00101\ A + 0.00638\ B + 0.000033\ C + 0.000002\ A*C - 0.000010\ B*C \quad (4.12)$$

4.2. Catalyst Optimization using ANOVA Analysis

With the ANOVA analysis completed, next step was to determine the best catalyst(s) for the production of biofuel grade compounds. Using the optimization tools, equations from 4.1 to 4.12 were solved side by side to maximize the ester production while keeping the final concentrations of organic acids, aldehydes, and other compounds minimum. For all three acid types used for peptizing, optimized preparation conditions were listed in Table 4.8.

Table 4.8. Optimized catalyst preparation conditions to maximize ester production

Code	Al Content (%)	Ni Content (%)	Calc. Temperature (°C)	Acid
D-01	25	0	900	HNO_3
D-02	25	0	900	H_2SO_4
D-03	75	20	900	H_3PO_4

In order to validate the optimization results, new catalysts were prepared following the calculated conditions. Under same reaction conditions as before, newly prepared catalysts were used in biofuel production experiment. Final product distribution was determined with GC-MS and listed in Table 4.9. Standard error values included in this table were calculated using the results obtained during the ANOVA analysis.

Table 4.9. GC-MS results of optimized catalyst final product distribution

	Aldehyde (%)	**Ester (%)**	**Org. Acid (%)**	**Others (%)**
0% Ni/25% Al_2O_3-75% SiO_2 w/HNO_3 at 900°C	11.20±1.32%	35.50±1.25%	39.16±4.19%	14.15±8.99%
0% Ni/25% Al_2O_3-75% SiO_2 w/H_2SO_4 at 900°C	31.66±8.28%	33.38±9.74%	11.45±1.82%	23.51±5.24%
20% Ni/75% Al_2O_3-25% SiO_2 w/H_3PO_4 at 900°C	4.92±0.81%	60.64±1.90%	27.99±1.85%	6.44±1.27%

To better visualize the results, values from Table 4.9 was plotted and was given in Figure 4.1. As it can be seen, using the 20% Ni/75% Al_2O_3-25% SiO_2 w/H_3PO_4 at 900°C catalyst gives the best ester production value of 60.64±0.65% compared to 11.20±0.46% and 31.66±2.85% ester production obtained with 0% Ni/25% Al_2O_3-75% SiO_2 w/HNO_3 at 900°C and 0% Ni/25% Al_2O_3-75% SiO_2 w/H_2SO_4 at 900°C catalysts, respectively. Low aldehyde and other compound yields indicate that the product selectivity during reaction favors the ester production. The downside of this catalyst is its

relatively high organic acid yield in the final biofuel mixture. High organic acid yield could be attributed to low reaction rate towards esters.

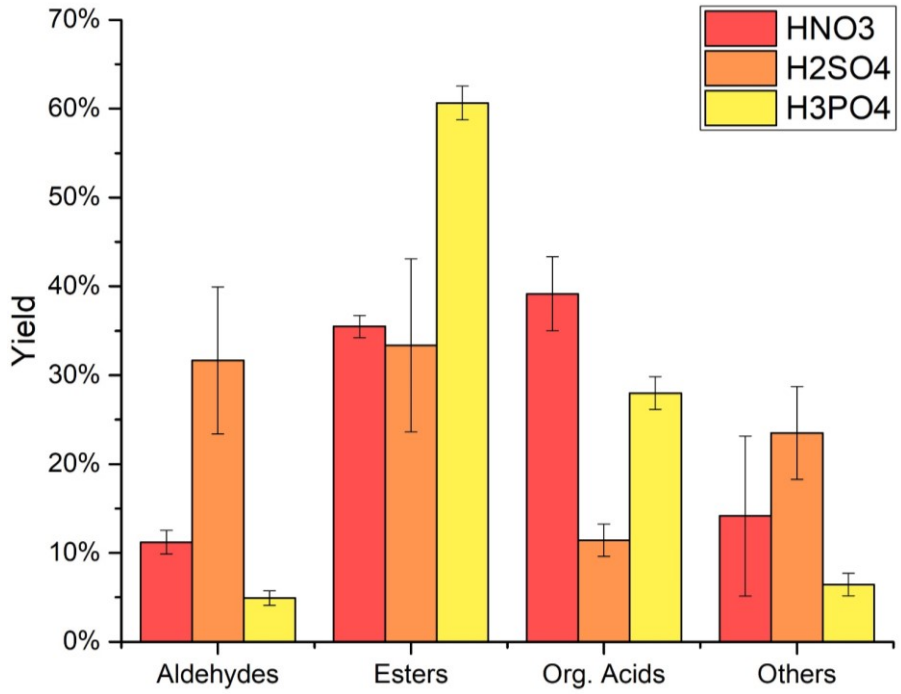

Figure 4.1. GC-MS final product distribution

While having an ester yield of 33.38±3.35%, 0% Ni/25% Al_2O_3-75% SiO_2 w/H_2SO_4 at 900ºC catalyst excels at very high organic acid utilization that can be seen with a very low organic acid yield of 11.45±0.63%. It is evident that organic acids reacted with this catalyst to produce aldehydes and other compounds since it gave the highest aldehyde and other compounds yield at the expense of ester yield.

Compared to other catalysts used in the statistical analysis, utilization of 0% Ni/25% Al_2O_3-75% SiO_2 w/HNO_3 at 900ºC was resulted in high ester yield compared to most of the catalysts. However, these results were downgraded when we compare it to optimized catalysts. While it gave higher ester yield, compared to 0% Ni/25% Al_2O_3-75% SiO_2 w/H_2SO_4 at 900ºC catalyst, 33.38±3.35%, looking at the error bars showed that there is no considerable difference between ester yields because both error bars intercept each other. Moreover, it performed worse than 0% Ni/25% Al_2O_3-75% SiO_2 w/H_2SO_4 at 900ºC catalyst with regards to aldehyde and other compound yields while giving the worst organic acid utilization even compared to 20% Ni/75% Al_2O_3-25% SiO_2 w/H_3PO_4 at 900ºC catalyst with a final organic acid yield of 39.16±1.44%.

All and all, from the optimization results, two catalysts, 20% Ni/75% Al_2O_3-25% SiO_2 w/H_3PO_4 at 900°C and 0% Ni/25% Al_2O_3-75% SiO_2 w/H_2SO_4 at 900°C showed promising results with respect to biofuel production. In the direct biofuel production perspective, 20% Ni/75% Al_2O_3-25% SiO_2 w/H_3PO_4 at 900°C catalyst gave the highest ester yield with the lowest aldehyde and other compounds, with low organic acid utilization as a downside. In raw material utilization perspective, 0% Ni/25% Al_2O_3-75% SiO_2 w/H_2SO_4 at 900°C gave the highest organic acid utilization with low ester yield and high aldehyde and other compounds yield. Further studies on these catalysts, both in reaction condition and catalyst composition state of the point, would further their performance immensely.

4.3. Catalyst Characterization

In order to understand the effect of crystal structure as well as its surface properties, selected catalysts were analyzed with XRD, BET, and NH_3-TPD. Since comparing catalysts prepared with different acids is like comparing apples and oranges, 10% Ni/25% Al_2O_3-75% SiO_2 w/HNO_3 at 500°C, 10% Ni/50% Al_2O_3-50% SiO_2 w/H_2SO_4 at 700°C, and 20% Ni/25% Al_2O_3-75% SiO_2 w/H_3PO_4 at 700°C catalysts were chosen for comparison purpose. Since these catalysts performed poorly during the experiments, having low ester yield while having low organic acid utilization, comparing these catalysts with optimized catalysts could shine a light on the reason why optimized catalysts performed better than other catalysts.

4.3.1. X-Ray Diffraction Analysis

X-Ray diffraction analysis showed that in none of the catalysts which contains nickel in their composition, 10% Ni/25% Al_2O_3-75% SiO_2 w/HNO_3 at 500°C, 10% Ni/50% Al_2O_3-50% SiO_2 w/H_2SO_4 at 700°C, 20% Ni/25% Al_2O_3-75% SiO_2 w/H_3PO_4 at 700°C, and 20% Ni/75% Al_2O_3-25% SiO_2 w/H_3PO_4 at 900°C, there was neither Ni nor NiO peaks observed, (43.29° for Ni and 44.50 for NiO) regardless of nickel loading, calcination temperature or acid type. (Richardson, Scates, and Twigg 2003) Lack of nickel crystals in the XRD indicates that the crystallite size of the nickel is smaller than 5 nm, which is the lower detection limit of XRD. Low-angle XRD can be used to determine the nickel size. (Cullity and Weymouth 1957)

Table 4.10. XRD crystal sizes and crystal phases for selected catalysts

Catalyst Name	Code	1st Crystal Position / Size / Phase (2θ/nm/(hkl)	2nd Crystal Position / Size/ Phase (2θ/nm/(hkl)	3rd Crystal Position / Size / Phase (2θ/nm/(hkl)	Average Crystalline Size (nm)	Crystal Name / Reference No
10% Ni/25% Al_2O_3-75% SiO_2 w/HNO_3 at 500°C	A-05	No peaks observed. XRD Amorphous Structure				
0% Ni/25% Al_2O_3-75% SiO_2 w/HNO_3 at 900°C	D-01	No peaks observed. XRD Amorphous Structure				
10% Ni/50% Al_2O_3-50% SiO_2 w/H_2SO_4 at 700°C	B-13	25.551 / 89.64 / (113)	30.758 / 53.98 / (024)	33.777 / (64.63) / (116)	69.42	Aluminum Sulphate / 00.022.0021
0% Ni/25% Al_2O_3-75% SiO_2 w/H_2SO_4 at 900°C	D-02	No peaks observed. XRD Amorphous Structure				
20% Ni/25% Al_2O_3-75% SiO_2 w/H_3PO_4 at 700°C	C-03	No peaks observed. XRD Amorphous Structure				
20% Ni/75% Al_2O_3-25% SiO_2 w/H_3PO_4 at 900°C	D-03	20.493 / 523.98 / (310)	25.995 / 313.84 / (400)	24.232 / 331.11 / (321)	389.64	Aluminum Phosphate / 00.013.0430

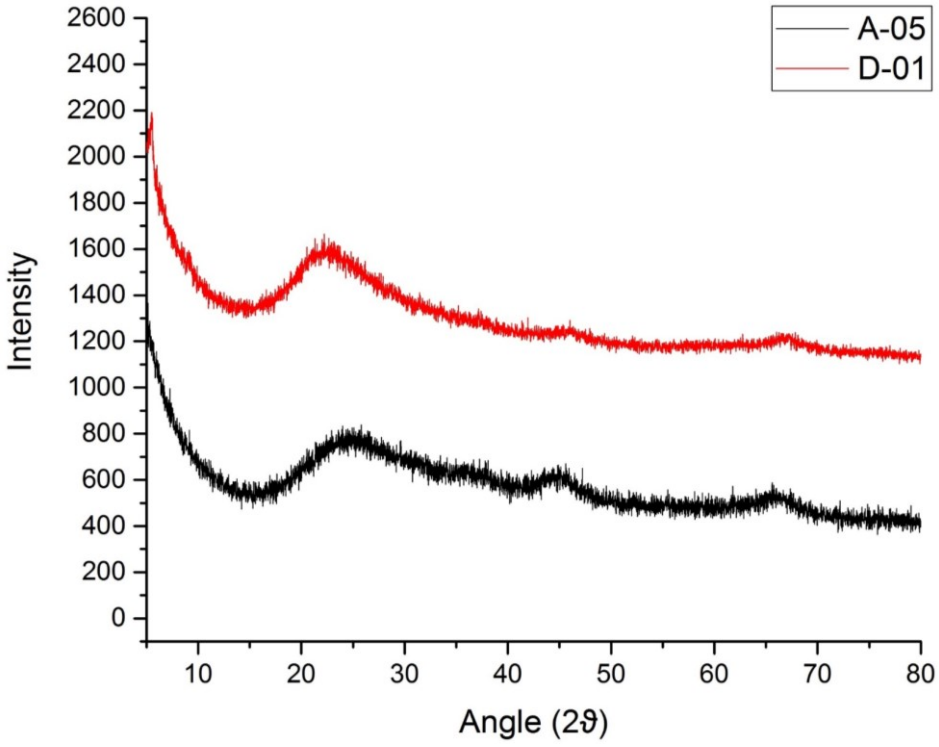

Figure 4.2. XRD spectra of selected catalysts prepared with HNO_3

Table 4.10 lists all the peaks observed from XRD spectra as well as the average crystallite size calculated by averaging three of the most abundant crystal phase using Eqn. 3.2. When XRD spectra of catalysts prepared with HNO_3 investigated, plotted in Figure 4.2, the amorphous structure was observed with both catalysts, meaning that no regular crystal structure was observed with XRD. The interaction between nickel and Al_2O_3-SiO_2 support in the 10% Ni/25% Al_2O_3-75% SiO_2 w/HNO_3 at 500°C (A-05) seems to increase the intensity of the peaks observed around 45° and 66°, indicating nickel has a positive effect on crystal formation.

While the effect of nickel addition for the catalysts prepared with HNO_3 could not be proven due to the lack of well-defined peaks, nickel addition triggers the crystal formation with catalysts prepared with H_2SO_4 that can be clearly seen in Figure 4.3. Even a low nickel loading of 10%, 10% Ni/50% Al_2O_3-50% SiO_2 w/H_2SO_4 at 700°C (B-13) catalyst shows Aluminum Sulphate ($Al_2(SO_4)_3$) which means acid used as the peptization agent modifies the Al_2O_3-SiO_2 support. Combining crystal phase analysis and product yields, shown in Table 4.2, it can be said that $Al_2(SO_4)_3$ crystallite phase is not suitable for biofuel production since it has low organic acid utilization and ester yields. Further analysis on this behavior, however, is required to proof this hypothesis. Opposite of this is true for 0% Ni/25% Al_2O_3-75% SiO_2 w/H_2SO_4 at 900°C catalyst that gave the highest

organic acid utilization while having no particular selectivity towards aldehydes, esters, and other compound yields despite having an amorphous structure. Moreover, the lack of selectivity can be explained with an amorphous structure. Many different sites on the catalyst surface promote different reaction routes without any pattern, resulting in high organic acid utilization and no selectivity.

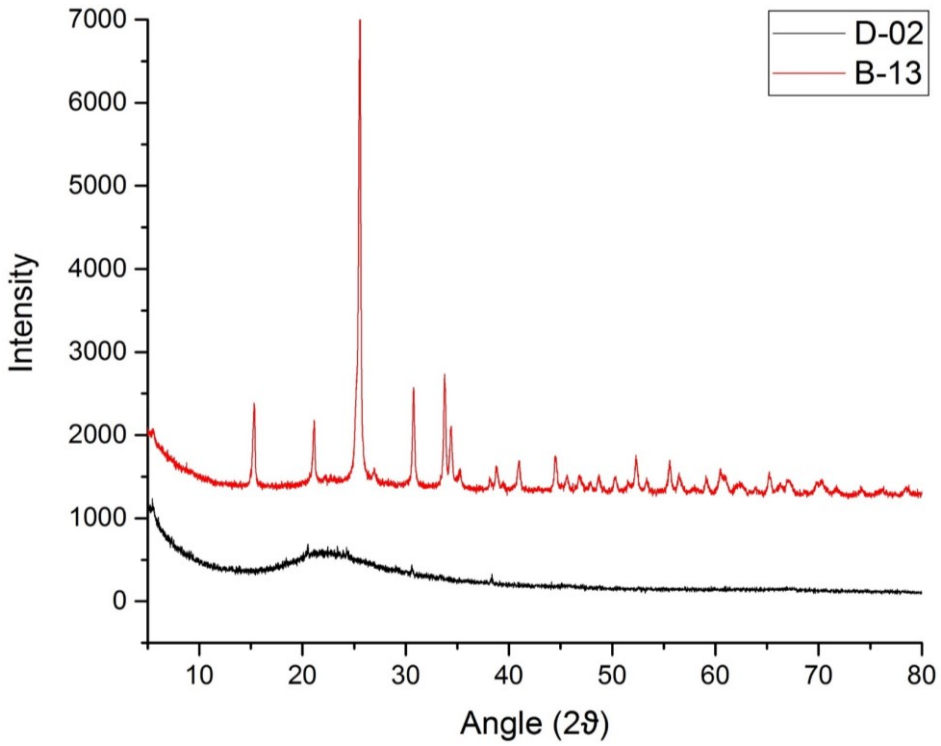

Figure 4.3. XRD spectra of selected catalysts prepared with H_2SO_4

XRD spectra for catalysts that were prepared with H_3PO_4 acid, shown in Figure 4.4, again shows one amorphous and one well-defined crystal structure. In this comparison, both catalysts have high nickel loading of 20%, while their aluminum composition and calcination temperature changing. Increased temperature and aluminum content promoted the Aluminum Phosphate ($Al_2(PO_4)_3$) crystal phase formation. Unlike the 0% Ni/25% Al_2O_3-75% SiO_2 w/H_2SO_4 at 900°C catalyst, the formation of $Al_2(PO_4)_3$ crystal phase with 20% Ni/75% Al_2O_3-25% SiO_2 w/H_3PO_4 at 900°C catalyst significantly increased the selectivity toward ester yield. That can be interpreted so that $Al_2(PO_4)_3$ crystal phase is the key to the formation of esters while without further analysis this is still a hypothesis. As it is listed in Table 4.10, the average crystal size of this catalyst is very high, 389.64 nm, which might affect on selectivity, however, this hypothesis requires further investigation on crystal size-selectivity interaction.

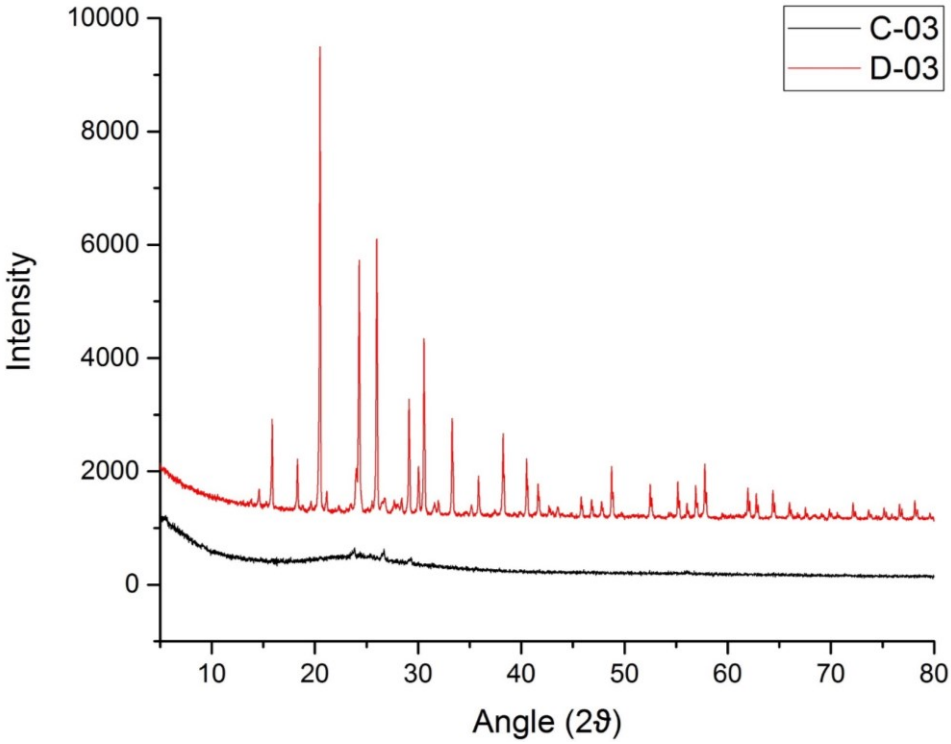

Figure 4.4. XRD spectra of selected catalysts prepared with H_3PO_4

4.3.2. TPD and BET Analysis

In order to understand the effect of acidic sites, as well as their strength, on the performance of selected catalysts, the NH_3-TPD analysis was conducted. Moreover, BET analysis was conducted for the determination of surface area, as well as pore size and pore structure of the catalysts. Summary of the results obtained with NH_3-TPD and BET analysis was listed in Table 4.11 while BET adsorption isotherms and, NH_3-TPD plots were given in Appendix D and Appendix E, respectively.

Analysis of BET surface area showed that 10% Ni/25% Al_2O_3-75% SiO_2 w/HNO_3 at 500ºC catalyst has the highest BET surface area. While increase in the calcination temperature resulted in lower BET surface area for the catalysts prepared with HNO_3, opposite is true for H_2SO_4 catalysts in which 0% Ni/25% Al_2O_3-75% SiO_2 w/H_2SO_4 at 900ºC catalyst having more than three times the surface area of 10% Ni/50% Al_2O_3-50% SiO_2 w/H_2SO_4 at 700ºC. Coupled with the lack of $Al_2(SO_4)_3$ peaks in the XRD plot given in Figure 4.3, it can be assumed that increase in the calcination temperature resulted in the release of SO_4^{2-} from the catalyst structure, which resulted with increasing in the catalyst surface area. Most intriguing results obtained with catalysts prepared with H_3PO_4

having the lowest surface area among while showing the highest selectivity towards esters.

From the adsorption isotherms of all catalysts shown in Appendix D, it can be said that all catalysts possess Type IV isotherms with Type A hysteresis loops. (Satterfield 1991) Similar isotherms between different catalysts that have vastly different catalytic performances towards biofuel production indicate that the catalyst surface is not a factor for the biofuel production.

Table 4.11. BET surface area and average pore volumes of selected catalysts

Catalyst Name	Bet Surface Area (m^2/g)	Average Pore Width (Å)	Adsorption Isotherm	NH_3-TPD Total Acid Sites (µmol/g)
10% Ni/25% Al_2O_3-75% SiO_2 w/HNO_3 at 500°C	**454.59**	**32.639**	**Type IV (Hysteresis A)**	**92.65**
0% Ni/25% Al_2O_3-75% SiO_2 w/HNO_3 at 900°C	**114.29**	**36.019**	**Type IV (Hysteresis A)**	**33.05**
10% Ni/50% Al_2O_3-50% SiO_2 w/H_2SO_4 at 700°C	**75.69**	**83.799**	**Type IV (Hysteresis A)**	**72.00**
0% Ni/25% Al_2O_3-75% SiO_2 w/H_2SO_4 at 900°C	**258.66**	**66.504**	**Type IV (Hysteresis A)**	**34.76**
20% Ni/25% Al_2O_3-75% SiO_2 w/H_3PO_4 at 700°C	**1.66**	**30.349**	**Type IV (Hysteresis A)**	**--**
20% Ni/75% Al_2O_3-25% SiO_2 w/H_3PO_4 at 900°C	**2.12**	**41.628**	**Type IV (Hysteresis A)**	**--**

To better visualize the NH_3-TPD results given in the Table 4.11, product distribution of all the selected catalysts plotted in Figure 4.5. NH_3-TPD total acid amounts

could not calculated for both 20% Ni/75% Al_2O_3-25% SiO_2 w/H_3PO_4 at 900ºC and 20% Ni/75% Al_2O_3-25% SiO_2 w/H_3PO_4 at 900ºC catalysts due to the low surface area of the catalysts, that can be seen in Table 4.11. Low surface area of these catalysts resulted with decrease in signal to noise ratio thus eliminating peak separation. (Figure E.3) Despite the lack of information about its acidity and acidic strength, it can be seen that 20% Ni/75% Al_2O_3-25% SiO_2 w/H_3PO_4 at 900ºC catalyst gave the highest selectivity towards esters with the second highest utilization of organic acid. Further analysis thus required to explain the activity and selectivity of this catalyst.

0% Ni/25% Al_2O_3-75% SiO_2 w/H_2SO_4 at 900ºC, given in Figure E.2, gave the highest organic acid utilization while having both strong and weak acid sites, higher than 400ºC and below 250ºC respectively.(Tanabe et al. 1990) This result implicates that strong acid sites are needed for the organic acid utilization. Moreover, by combining the aldehyde and other product yields to this information, it can be assumed that combination of weak and strong acid sites promotes various reaction pathways, resulting in high organic acid utilization with moderate selectivity towards ester production.

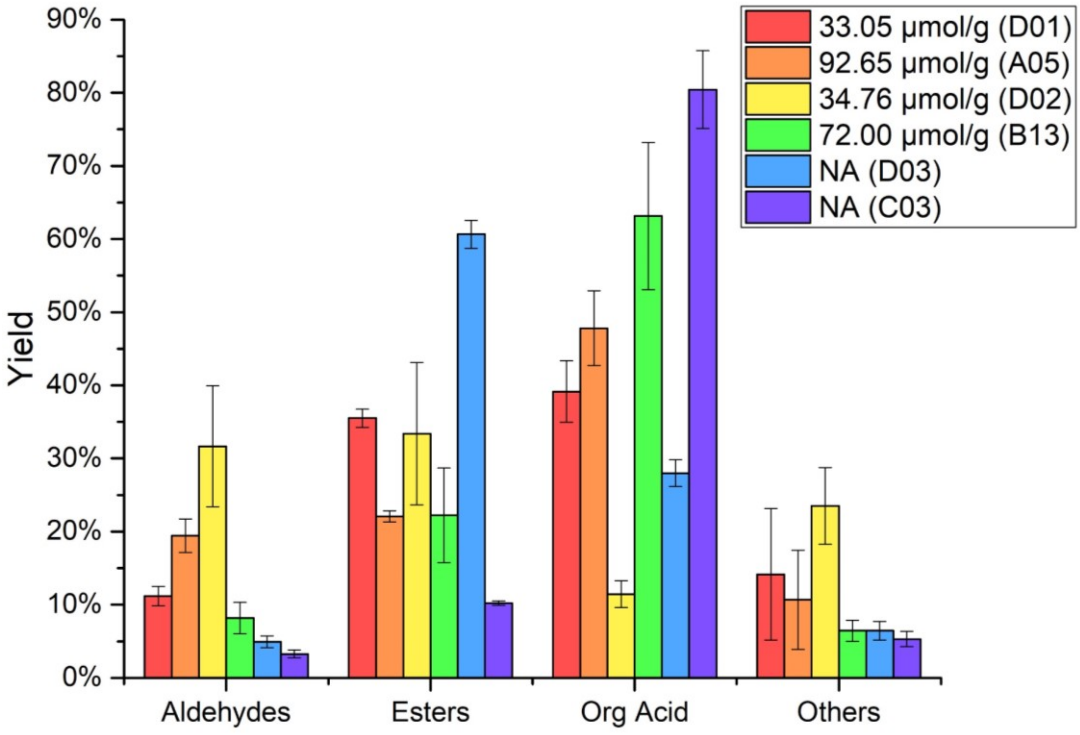

Figure 4.5. Product distribution of selected catalysts with their total acid amount

While very high acid amounts were observed for 10% Ni/25% Al_2O_3-75% SiO_2 w/HNO_3 at 500ºC and, 10% Ni/50% Al_2O_3-50% SiO_2 w/H_2SO_4 at 700ºC catalysts, they performed poorly during the reactions. Investigating the NH_3-TPD plots in Figure E.1 and Figure E.2 showed that these catalysts only possess weak acid sites from the peaks below 250ºC, indicating that organic acid cannot be reacted over weak acid sites.

All and all, a combination of all catalyst characterization showed that 20% Ni/75% Al_2O_3-25% SiO_2 w/H_3PO_4 at 900ºC catalyst was a very good candidate for biofuel production with highest ester selectivity while 0% Ni/25% Al_2O_3-75% SiO_2 w/H_2SO_4 at 900ºC catalyst gave the second-best performance with highest organic acid utilization with poor selectivity towards esters.

CHAPTER 5

CONCLUSION

During the study, heterogeneous nickel supported Al_2O_3-SiO_2 catalyst used for the production of biofuels from canola oil at low temperatures and atmospheric pressures. Experimental design principles applied to the study to investigate the effect of aluminum and nickel concentration, calcination temperature and acid type used in catalyst preparation on biofuel product distribution.

After ANOVA analyzes for each product type completed and empirical models constructed, best catalysts for ester yield with the lowest aldehyde and organic acid yield calculated to be 0% Ni/25% Al_2O_3-75% SiO_2 at 900^{o}C for catalysts prepared with HNO_3, H_2SO_4 and 20% Ni/75% Al_2O_3-25% SiO_2 at 900^{o}C for the catalyst prepared with H_3PO_4. Validation experiments with model optimized catalysts showed that 20% Ni/75% Al_2O_3-25% SiO_2 at 900^{o}C catalyst prepared with H_3PO_4 gave the highest ester yield with 60.64%±0.65% with moderate organic acid content of 27.99%±0.64% while 0% Ni/25% Al_2O_3-75% SiO_2 at 900^{o}C catalyst prepared with H_2SO_4 gave the lowest organic acid yield of 11.45%±0.63% with moderate ester yield of 33.38%±0.63%.

XRD results indicated that selectivity attributed to 20% Ni/75% Al_2O_3-25% SiO_2 w/H_3PO_4 at 900^{o}C catalyst could be traced to the presence of $Al_2(PO_4)_3$ crystal phase. NH_3-TPD results showed that vegetable oil utilization occurred over strong acid sites while the combination of weak and strong acid sites resulted with high organic acid utilization and product mixture containing equal parts of esters, aldehydes, and other products. Results also showed that nature of the acid sites, meaning the strength of the acid sites, was much more important than the sheer amount of acid sites, indicated by the poor performance of 10% Ni/25% Al_2O_3-75% SiO_2 w/HNO_3 at 500^{o}C and, 10% Ni/50% Al_2O_3-50% SiO_2 w/H_2SO_4 at 700^{o}C catalysts.

REFERENCES

Alenezi, R., M. Baig, J. Wang, R. Santos, and G. A. Leeke. 2010. "Continuous Flow Hydrolysis of Sunflower Oil for Biodiesel." *Energy Sources Part a-Recovery Utilization and Environmental Effects* 32 (5):460-468. doi: 10.1080/15567030802612341.

Apostolakou, A. A., I. K. Kookos, C. Marazioti, and K. C. Angelopoulos. 2009. "Techno-economic analysis of a biodiesel production process from vegetable oils." *Fuel Processing Technology* 90 (7-8):1023-1031. doi: 10.1016/j.fuproc.2009.04.017.

Atabani, A. E., A. S. Silitonga, H. C. Ong, T. M. I. Mahlia, H. H. Masjuki, I. A. Badruddin, and H. Fayaz. 2013. "Non-edible vegetable oils: A critical evaluation of oil extraction, fatty acid compositions, biodiesel production, characteristics, engine performance and emissions production." *Renewable & Sustainable Energy Reviews* 18:211-245. doi: 10.1016/j.rser.2012.10.013.

BP. 2017. "BP Statistical Review of World Energy 2017." BP P.L.C, accessed 01.08.2017. https://www.bp.com/content/dam/bp/en/corporate/pdf/energy-economics/statistical-review-2017/bp-statistical-review-of-world-energy-2017-full-report.pdf.

Bugarski, A. D., J. A. Hummer, and S. Vanderslice. 2016. "Effects of hydrotreated vegetable oil on emissions of aerosols and gases from light-duty and medium-duty older technology engines." *J Occup Environ Hyg* 13 (4):293-302. doi: 10.1080/15459624.2015.1116695.

Corro, Grisel, Nallely Tellez, Teresita Jimenez, Armando Tapia, Fortino Banuelos, and Odilón Vazquez-Cuchillo. 2011. "Biodiesel from waste frying oil. Two step process using acidified SiO 2 for esterification step." *Catalysis today* 166 (1):116-122.

Cullity, Bernard Dennis, and John W Weymouth. 1957. "Elements of X-ray Diffraction." *American Journal of Physics* 25 (6):394-395.

Deka, Ramesh Ch. 1998. "Acidity in zeolites and their characterization by different spectroscopic methods."

Dickerson, T., and J. Soria. 2013. "Catalytic Fast Pyrolysis: A Review." *Energies* 6 (1):514-538. doi: 10.3390/en6010514.

EEA. 2017. "Greenhouse gas emissions by sector." Eurostat, accessed 01.08.2017. http://ec.europa.eu/eurostat/web/products-datasets/-/tsdcc210.

Endalew, A. K., Y. Kiros, and R. Zanzi. 2011. "Inorganic heterogeneous catalysts for biodiesel production from vegetable oils." *Biomass & Bioenergy* 35 (9):3787-3809. doi: 10.1016/j.biombioe.2011.06.011.

EPA. 2016. "Climate change indicators in the United States." U.S. Environmental Protection Agency, accessed 12.08.2017. www.epa.gov/climate-indicators.

EUComm. 2013. "The Clean Air Policy Package." European Commission Environment, accessed 28.07.2017. http://ec.europa.eu/environment/air/clean_air_policy.htm.

EUComm. 2014. "Alternative fuels for sustainable mobility in Europe." European Commision Transportation, accessed 28.07.2017. https://ec.europa.eu/transport/themes/urban/cpt_en.

Galadima, Ahmad, and Oki Muraza. 2015. "Catalytic upgrading of vegetable oils into jet fuels range hydrocarbons using heterogeneous catalysts: A review." *Journal of Industrial and Engineering Chemistry* 29:12-23.

Hermida, L., A. Z. Abdullah, and A. R. Mohamed. 2015. "Deoxygenation of fatty acid to produce diesel-like hydrocarbons: A review of process conditions, reaction kinetics and mechanism." *Renewable & Sustainable Energy Reviews* 42:1223-1233. doi: 10.1016/j.rser.2014.10.099.

Jain, S., and M. P. Sharma. 2010. "Biodiesel production from Jatropha curcas Oil." *Renewable & Sustainable Energy Reviews* 14 (9):3140-3147. doi: 10.1016/j.rser.2010.07.047.

Khan, N. A., and H. el Dessouky. 2009. "Prospect of biodiesel in Pakistan." *Renewable & Sustainable Energy Reviews* 13 (6-7):1576-1583. doi: 10.1016/j.rser.2008.09.016.

Leung, Dennis Y. C., Xuan Wu, and M. K. H. Leung. 2010. "A review on biodiesel production using catalyzed transesterification." *Applied Energy* 87 (4):1083-1095. doi: http://dx.doi.org/10.1016/j.apenergy.2009.10.006.

Leung, DYC, and Y Guo. 2006. "Transesterification of neat and used frying oil: optimization for biodiesel production." *Fuel Processing Technology* 87 (10):883-890.

Liu, Yingying, Houfang Lu, Changjun Liu, and Bin Liang. 2008. "Solubility measurement for the reaction systems in pre-esterification of high acid value Jatropha curcas L. oil." *Journal of Chemical & Engineering Data* 54 (5):1421-1425.

Loe, Ryan, Eduardo Santillan-Jimenez, Tonya Morgan, Lilia Sewell, Yaying Ji, Samantha Jones, Mark A Isaacs, Adam F Lee, and Mark Crocker. 2016. "Effect of Cu and Sn promotion on the catalytic deoxygenation of model and algal lipids to fuel-like hydrocarbons over supported Ni catalysts." *Applied Catalysis B: Environmental* 191:147-156.

Montgomery, Douglas C. 2014. "Textbook: Design and Analysis of Experiments."

Murata, Kazuhisa, Yanyong Liu, Megumu Inaba, and Isao Takahara. 2010. "Production of synthetic diesel by hydrotreatment of jatropha oils using Pt− Re/H-ZSM-5 catalyst." *Energy & Fuels* 24 (4):2404-2409.

Pinzi, S., I. L. Garcia, F. J. Lopez-Gimenez, M. D. L. de Castro, G. Dorado, and M. P. Dorado. 2009. "The Ideal Vegetable Oil-based Biodiesel Composition: A Review of Social, Economical and Technical Implications." *Energy & Fuels* 23 (5):2325-2341. doi: 10.1021/ef801098a.

Rashid, Umer, and Farooq Anwar. 2008. "Production of biodiesel through optimized alkaline-catalyzed transesterification of rapeseed oil." *Fuel* 87 (3):265-273.

Richardson, James T, Robert Scates, and Martyn V Twigg. 2003. "X-ray diffraction study of nickel oxide reduction by hydrogen." *Applied Catalysis A: General* 246 (1):137-150.

Satterfield, Charles N. 1991. "Heterogeneous catalysis in industrial practice."

Shahid, E. M., and Y. Jamal. 2011. "Production of biodiesel: A technical review." *Renewable & Sustainable Energy Reviews* 15 (9):4732-4745. doi: 10.1016/j.rser.2011.07.079.

Stedile, T., L. Ender, H. F. Meier, E. L. Simionatto, and V. R. Wiggers. 2015. "Comparison between physical properties and chemical composition of bio-oils derived from lignocellulose and triglyceride sources." *Renewable & Sustainable Energy Reviews* 50:92-108. doi: 10.1016/j.rser.2015.04.080.

Tanabe, Kozo, Makoto Misono, H Hattori, and Yoshio Ono. 1990. *New solid acids and bases: their catalytic properties*. Vol. 51: Elsevier.

Thomas, John Meurig, and W John Thomas. 2014. *Principles and practice of heterogeneous catalysis*: John Wiley & Sons.

Toba, Makoto, Yohko Abe, Hidetoshi Kuramochi, Masahiro Osako, T Mochizuki, and Yuji Yoshimura. 2011. "Hydrodeoxygenation of waste vegetable oil over sulfide catalysts." *Catalysis Today* 164 (1):533-537.

TurkStat. 2015. "National greenhouse gas inventory report 1990-2013." Turkish Statistical Institute, accessed 01.08.2017. http://www.turkstat.gov.tr/PreHaberBultenleri.do?id=18744.

Van Gerpen, Jon. 2005. "Biodiesel processing and production." *Fuel processing technology* 86 (10):1097-1107.

Van Gerpen, Jon, B Shanks, Rudy Pruszko, D Clements, and G Knothe. 2004. "Biodiesel analytical methods." *National Renewable Energy Laboratory, Colorado*:37-47.

Veriansyah, Bambang, Jae Young Han, Seok Ki Kim, Seung-Ah Hong, Young Jun Kim, Jong Sung Lim, Young-Wong Shu, Seong-Geun Oh, and Jaehoon Kim. 2012. "Production of renewable diesel by hydroprocessing of soybean oil: Effect of catalysts." *Fuel* 94:578-585.

Vu, Hoan X, Matthias Schneider, Ursula Bentrup, Tung T Dang, Binh MQ Phan, Duc A Nguyen, Udo Armbruster, and Andreas Martin. 2015. "Hierarchical ZSM-5 materials for an enhanced formation of gasoline-range hydrocarbons and light olefins in catalytic cracking of triglyceride-rich biomass." *Industrial & Engineering Chemistry Research* 54 (6):1773-1782.

Xu, Junming, Jianchun Jiang, and Jiaping Zhao. 2016. "Thermochemical conversion of triglycerides for production of drop-in liquid fuels." *Renewable and Sustainable Energy Reviews* 58:331-340.

Yenumala, S. R., S. K. Maity, and D. Shee. 2016. "Hydrodeoxygenation of karanja oil over supported nickel catalysts: influence of support and nickel loading." *Catalysis Science & Technology* 6 (9):3156-3165. doi: 10.1039/c5cy01470k.

Yoldas, Bulent E. 1975. "Alumina gels that form porous transparent Al 2 O 3." *Journal of Materials Science* 10 (11):1856-1860.

Yusuf, N. N. A. N., S. K. Kamarudin, and Z. Yaakub. 2011. "Overview on the current trends in biodiesel production." *Energy Conversion and Management* 52 (7):2741-2751. doi: 10.1016/j.enconman.2010.12.004.

APPENDIX A

GC-MS DETECTED COMPOUND LIST

Table A.1. Liquid phase GC-MS detected compounds with their group and retention times

Formula	Compound Name	Group	Time (min)
C6H12O	Hexanal	Aldehyde	4.424
C7H12O	2-Heptenal, (Z)-	Aldehyde	8.169
C9H12	Benzene, 1,2,4-trimethyl-	Other	8.376
C9H14O	Furan, 2-pentyl-	Other	8.843
C6H12O2	Hexanoic acid	Organic Acid	9.021
C8H16O	Octanal	Aldehyde	9.078
C7H10O	2,4-Heptadienal, (E,E)-	Aldehyde	9.256
C8H14O	2-Octenal, (E)-	Aldehyde	10.101
C12H22O3	Hexanoic acid, anhydride	Organic Acid	10.207
C10H22O2	Hexane, 1,1-diethoxy-	Other	10.659
C9H18O	Nonanal	Aldehyde	10.885
C9H14O	2,6-Nonadienal, (E,Z)-	Aldehyde	11.7
C9H16O	2-Nonenal, (E)-	Aldehyde	11.795
C10H20O	Decanal	Aldehyde	12.496
C10H18O	2-Decenal, (Z)-	Aldehyde	13.122
C9H18O2	Nonanoic acid	Organic Acid	13.595
C10H16O	2,4-Decadienal, (E,E)-	Aldehyde	13.799
C11H20O3	4-Nonanone, 7-ethyl-	Other	14.715
C11H20O	2-Undecenal	Aldehyde	14.748
C12H22O	: 2-Butyl-2,7-octadien-1-ol	Other	14.837
C10H20O	3-Decen-1-ol, (Z)-	Other	14.941
C7H12O	4-Heptenal	Aldehyde	15.017
C15H32	Pentadecane	Other	16.452
C17H34	8-Heptadecene	Other	18.544
C20H40O	3,7,11,15-Tetramethyl-2-hexadecen-1-ol	Other	20.237
C20H40O2	9-Octadecene, 1,1-dimethoxy-, (Z)-	Other	20.749
C16H32O2	n-Hexadecanoic acid	Organic Acid	21.569
C18H36O2	Hexadecanoic acid, ethyl ester	Ester	21.83
C18H34O	9-Octadecenal, (Z)-	Aldehyde	21.873
C18H34O2	Oleic Acid	Organic Acid	22.658
C20H38O2	(E)-9-Octadecenoic acid ethyl ester	Ester	23.463
C35H68O5	Hexadecanoic acid, 1-(hydroxymethyl)-1,2-ethanediyl ester	Ester	24.589

(Cont. in next page)

Table A.1. Cont.

Formula	Compound Name	Group	Time (min)
C21H40O4	9-Octadecenoic acid (Z)-, 2-hydroxy-1-(hydroxymethyl)ethyl ester	Ester	25.521
C36H70O3	Stearic anhydride	Ester	25.943
C28H44O4	9-Octadecenoic acid, (2-phenyl-1,3-dioxolan-4-yl)methyl ester, cis-	Ester	26.176
C26H50	11-Hexacosyne	Other	26.652
C20H40O2	Ethanol, 2-(9-octadecenyloxy)-, (Z)-	Other	26.71
C29H58O2	Heptanoic acid, docosyl ester	Ester	27.395
C39H76O3	Oleic acid, 3-(octadecyloxy)propyl ester	Ester	29.305
C28H46O	Ergosta-7,22-dien-3-ol, (3á,22E)-	Other	29.811
C37H76O	1-Heptatriacotanol	Other	29.933
C26H44O5	Ethyl iso-allocholate	Other	30.19
C30H50O2	Ergost-5-en-3-ol, acetate, (3á,24R)-	Other	30.663
C47H82O2	Stigmast-5-en-3-ol, oleate	Other	31.295
C47H82O2	Stigmastan-3,5-diene	Other	31.759
C28H48O	Campesterol	Other	33.608
C29H50O	ç-Sitosterol	Other	34.743
C57H104O6	9-Octadecenoic acid, 1,2,3-propanetriyl ester, (E,E,E)-	Ester	39.356

APPENDIX B

RESIDUAL PLOTS

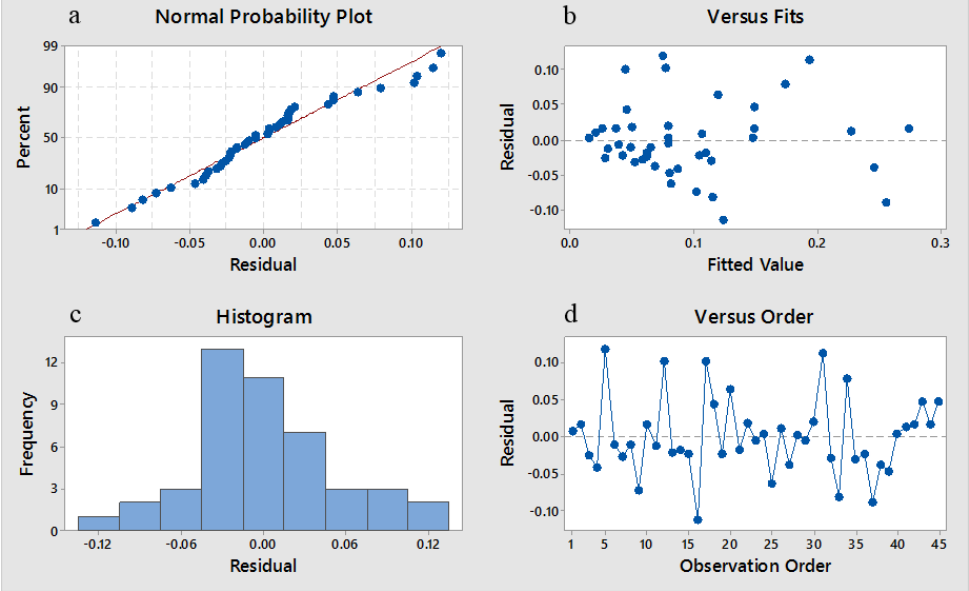

Figure B.1. Residual plots for aldehyde yield a) normal probability plot b) residual vs fitted (calculated) values c) histogram analysis of residuals d) distribution of residual according to run order

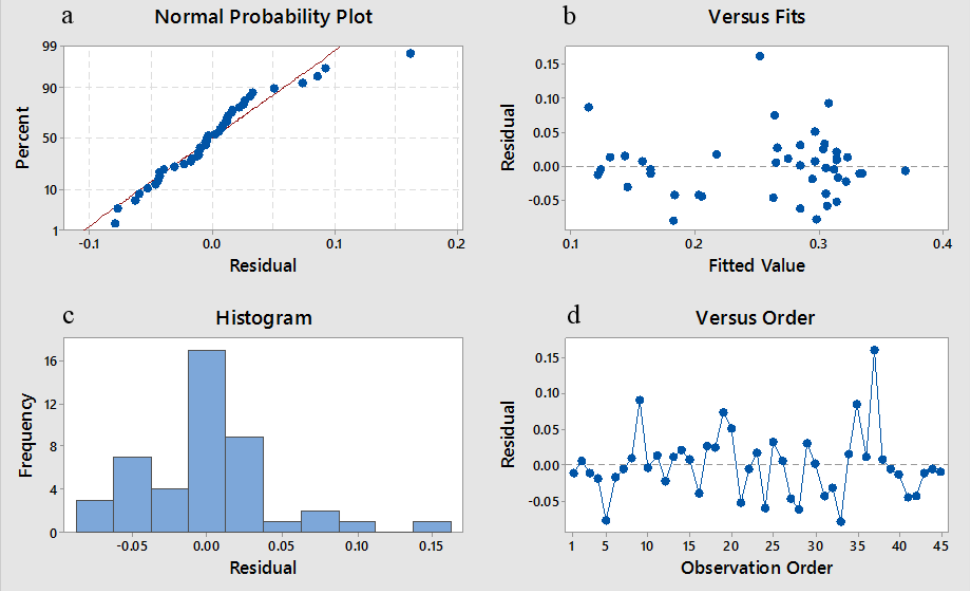

Figure B.2.Residual plots for ester yield a) normal probability plot b) residual vs fitted (calculated) values c) histogram analysis of residuals d) distribution of residual according to run order

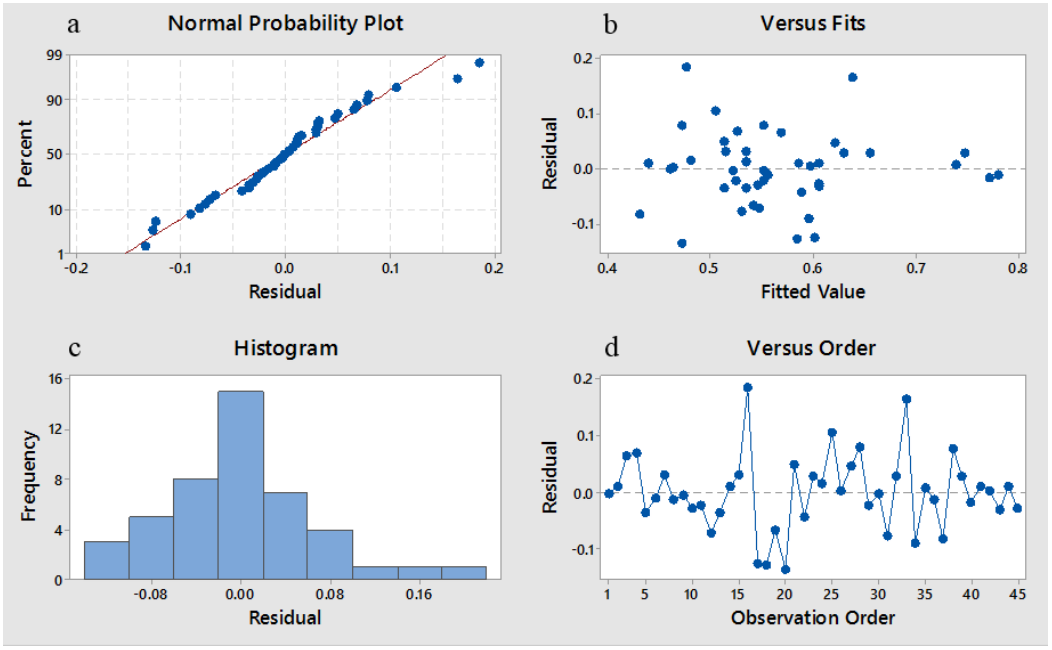

Figure B.3. Residual plots for organic acids yield a) normal probability plot b) residual vs fitted (calculated) values c) histogram analysis of residuals d) distribution of residual according to run order

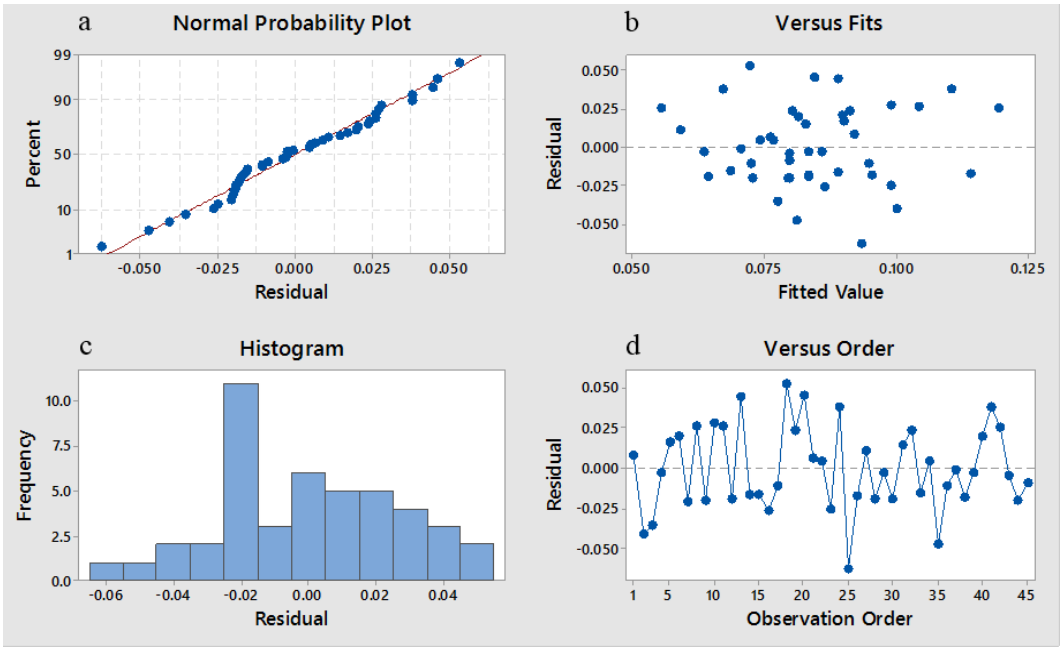

Figure B.4. Residual plots for others yield a) normal probability plot b) residual vs fitted (calculated) values c) histogram analysis of residuals d) distribution of residual according to run order

APPENDIX C

MODEL COEFFICIENT CALCULATION AND MODEL SUMMARY

Table C.1. T-Value calculations for the determination of the constants used in the model equation for aldehyde yield

Term	Effect	Coef	SE Coef	T-Value	P-Value	VIF
Constant		0.09658	0.00863	11.2	0	
A	-0.0103	-0.0052	0.0118	-0.44	0.664	1
B	-0.0091	-0.0045	0.0118	-0.38	0.703	1
C	0.0392	0.0196	0.0118	1.66	0.106	1
D						
H2SO4	-0.0345	-0.0173	0.0122	-1.42	0.166	1.33
H3PO4	0.1049	0.0525	0.0122	4.3	0	1.33
A*B	0.0698	0.0349	0.0167	2.09	0.044	1
B*C	0.0567	0.0284	0.0167	1.7	0.098	1
C*D						
H2SO4	-0.1096	-0.0548	0.0167	-3.28	0.002	1.33
H3PO4	0.165	0.0825	0.0167	4.94	0	1.33

Table C.2. T-Value calculations for the determination of the constants used in the model equation for ester yield

Term	Effect	Coef	SE Coef	T-Value	P-Value	VIF
Constant		0.25445	0.00747	34.08	0	
A	-0.0387	-0.0193	0.0102	-1.89	0.067	1
B	-0.002	-0.001	0.0102	-0.1	0.921	1
C	0.0188	0.0094	0.0102	0.92	0.364	1
D						
H2SO4	0.0612	0.0306	0.0106	2.9	0.006	1.33
H3PO4	-0.1818	-0.0909	0.0106	-8.61	0	1.33
A*C	-0.0563	-0.0282	0.0145	-1.95	0.059	1
C*D						
H2SO4	-0.06	-0.03	0.0145	-2.08	0.045	1.33
H3PO4	0.0631	0.0316	0.0145	2.18	0.036	1.33

Table C.3. T-Value calculations for the determination of the constants used in the model equation for organic acid yield

Term	Effect	Coef	SE Coef	T-Value	P-Value	VIF
Constant		0.5639	0.0109	51.58	0	
A	0.0411	0.0205	0.015	1.37	0.179	1
B	0.0239	0.012	0.015	0.8	0.429	1
C	-0.0631	-0.0315	0.015	-2.11	0.042	1
D						
H2SO4	-0.0253	-0.0127	0.0155	-0.82	0.418	1.33
H3PO4	0.083	0.0415	0.0155	2.69	0.011	1.33
A*B	-0.0838	-0.0419	0.0212	-1.98	0.055	1
C*D						
H2SO4	0.179	0.0895	0.0212	4.23	0	1.33
H3PO4	-0.2443	-0.1221	0.0212	-5.77	0	1.33

Table C.4. T-Value calculations for the determination of the constants used in the model equation for other compound yield

Term	Effect	Coef	SE Coef	T-Value	P-Value	VIF
Constant		0.08399	0.00424	19.8	0	
A	0.00817	0.00408	0.00581	0.7	0.486	1
B	-0.01435	-0.00718	0.00581	-1.24	0.224	1
C	0.00615	0.00307	0.00581	0.53	0.6	1
D						
H2SO4	-0.00126	-0.00063	0.006	-0.11	0.917	1.33
H3PO4	-0.00841	-0.0042	0.006	-0.7	0.488	1.33
A*C	0.01669	0.00835	0.00821	1.02	0.316	1
B*C	-0.04055	-0.02027	0.00821	-2.47	0.018	1

Table C.5. R^2 and R^2(adjusted) values for empirical model summary calculated for aldehyde, ester, organic acid and other compound yield in the product

	R^2	R^2(adjusted)
Aldehyde	61.03%	51.01%
Ester	71.66%	65.37%
Organic Acid	60.07%	51.19%
Others	21.60%	6.77%

APPENDIX D

BET ADSORPTION-DESORPTION ISOTHERMS

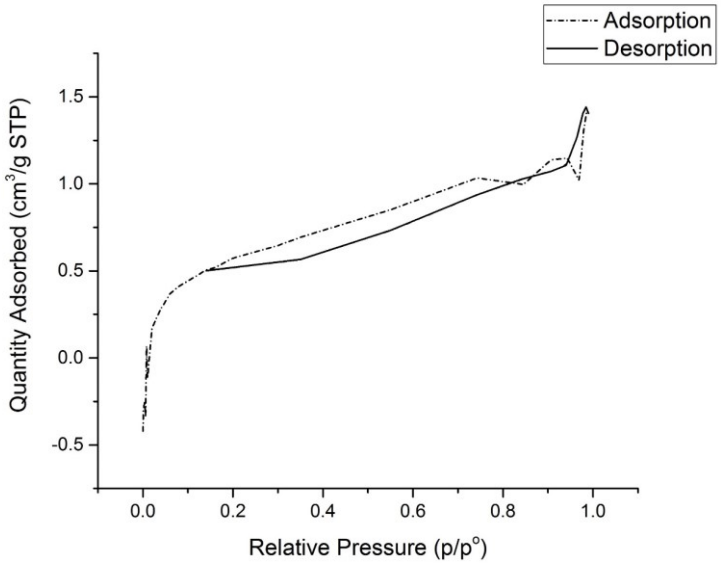

Figure D.1. BET adsorption-desorption isotherms for 10% Ni/25% Al_2O_3-75% SiO_2 w/HNO_3 at 500°C

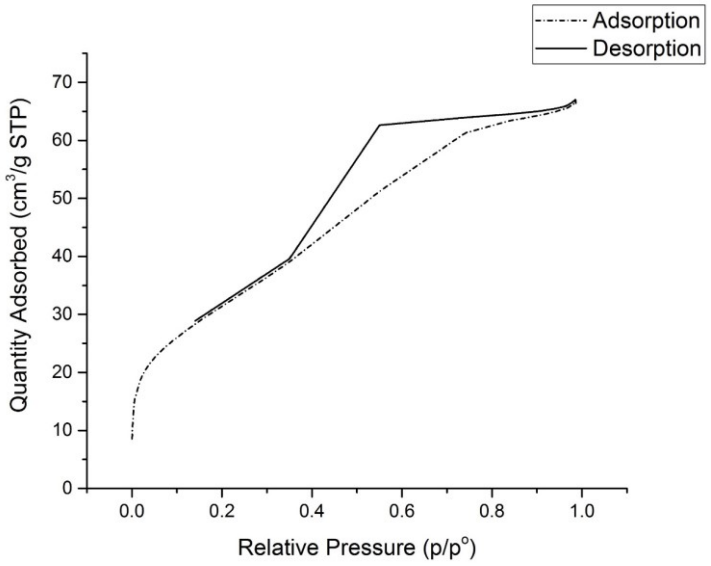

Figure D.2. BET adsorption-desorption isotherms for 0% Ni/25% Al_2O_3-75% SiO_2 w/HNO_3 at 900°C

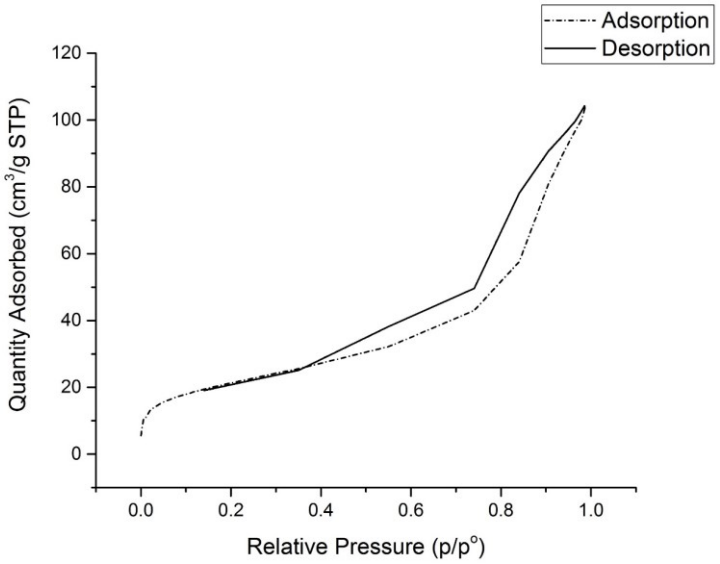

Figure D.3. BET adsorption-desorption isotherms for 10% Ni/50% Al_2O_3-50% SiO_2 w/H_2SO_4 at 700°C

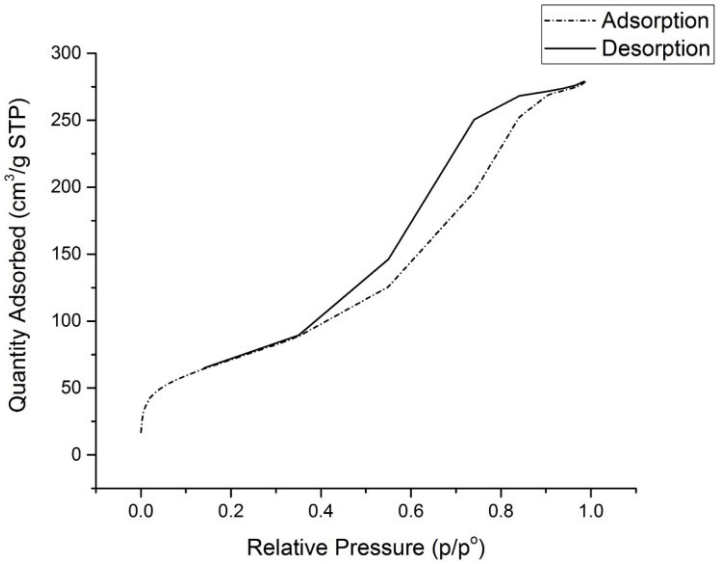

Figure D.4. BET adsorption-desorption isotherms for 0% Ni/25% Al_2O_3-75% SiO_2 w/H_2SO_4 at 900°C

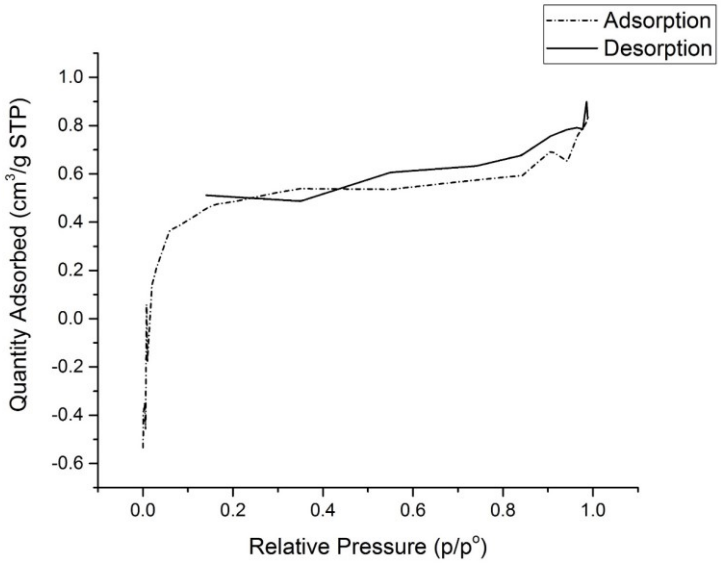

Figure D.5. BET adsorption-desorption isotherms for 20% Ni/25% Al_2O_3-75% SiO_2 w/H_3PO_4 at 700°C

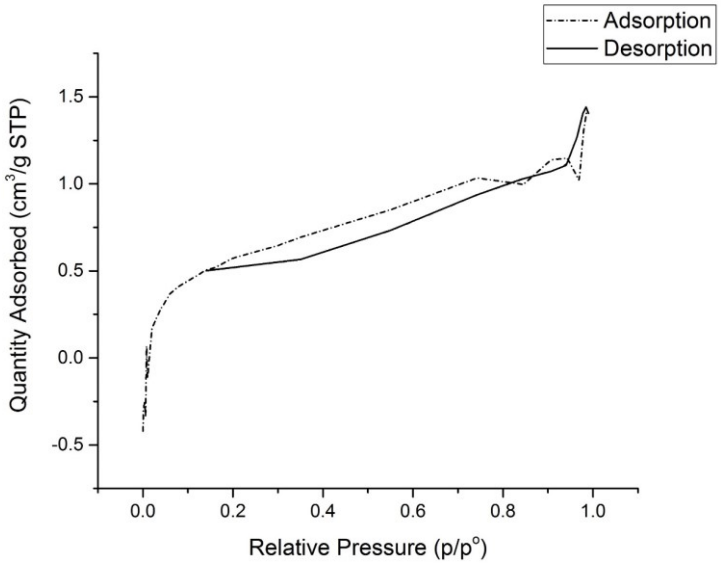

Figure D.6. BET adsorption-desorption isotherms for 20% Ni/75% Al_2O_3-25% SiO_2 w/H_3PO_4 at 900°C

APPENDIX E

NH_3-TPD PLOTS

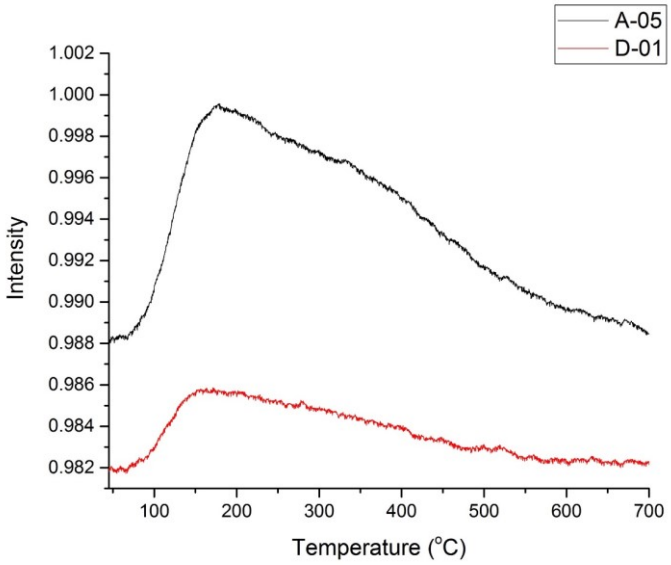

Figure E.1. NH_3-TPD plot of selected catalysts prepared with HNO_3

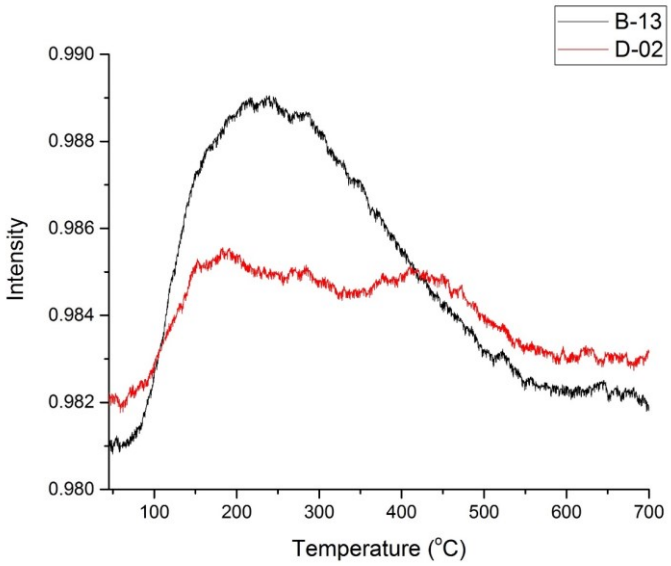

Figure E.2. NH_3-TPD plot of selected catalysts prepared with H_2SO_4

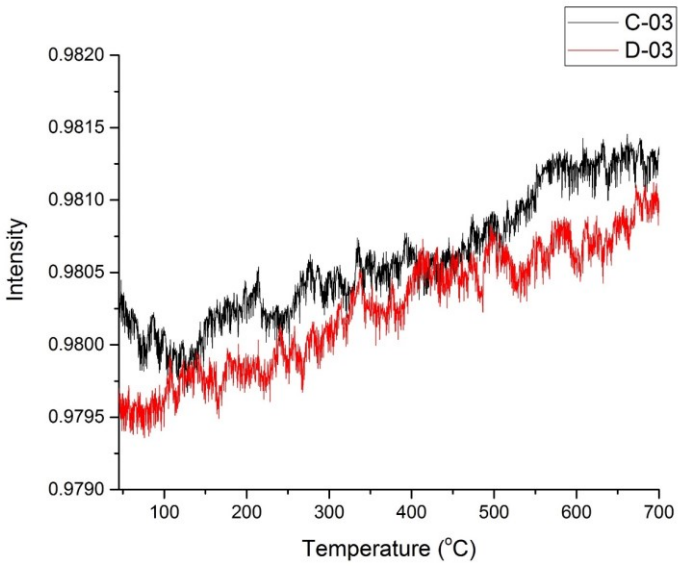

Figure E.3. NH_3-TPD plot of selected catalysts prepared with H_3PO_4